

Dear Editors and Reviewers:

Thanks very much for your letter and for the reviewers' comments concerning our manuscript entitled "Detecting seasonal and long-term vertical deformation in the North China Plain using GRACE and GPS" (No. hess-2016-552). Those comments are all valuable and very helpful for revising and improving our paper, as well as the important guiding significance to our researches. We have studied comments carefully and have made major revision which we hope to meet with approval. Revised portions are marked in the "Marked-up manuscript version". The main corrections in the paper and the responses to the reviewer's comments are as following.

Part I . Responses to the comments

Anonymous Referee #1 (Received and published: 18 November 2016)

In this manuscript, the authors present the time series variation of vertical displacement in North China Plain using GPS and GRACE data. Also, they analyzed the impact of Terrestrial Water Storage loss on vertical displacement. Generally, the manuscript is written clearly and illustrates some interesting results about the long-term variation of vertical displacement in North China Plain from 2003 to 2013 and discussion about the impact factors of vertical displacement like TWS loss. However, the manuscript suffers some deficiencies that need to be discussed before publishing of the manuscript. The major points that need to be added are provided

below.

Dear Anonymous Referee #1,

Thanks very much for your constructive comments. We have studied comments carefully and here replied each comment bellow. The original comments are in plain text and the replies in italics which we hope meet with approval.

1) Surface vertical displacement and estimation of water storage variation using GRACE data were presented in many researches during recent years and the methodology are more or less the same. However, there is little discussion in validation of the result. In this study, is there any field measurement data of groundwater level for validation of the water storage loss in NCP?

>Linsong Wang et al.: Thank you very much for the good comments that you mentioned our study result need more discuss, basing on measurement data of groundwater level in NCP. We have acquired in-situ groundwater level measurements (available only from 2002 to 2013), which are mainly located in the central and eastern plain of NCP (including the Beijing and Tianjin city, some cities of Hebei Henan and Shandong province) and are obtained from Ministry of Water Resources of China (available at: <http://sqqx.hydroinfo.gov.cn/shuiziyuan/>). We also collected the daily precipitation data (rainfall amount) for weather stations during the period of 2003–2012 from China Meteorological Data Sharing Service System (CMDSSS) (available at: <http://cdc.cma.gov.cn/index.jsp>). In revised manuscript, we have get the

area-weighted mean groundwater level change series in the NCP from time series of monthly groundwater table depth changes of 20 cities in our study region (Figure 7 in revised manuscript). Using the mean time series of monthly groundwater level data, we can compare the rate of loss between groundwater storage (GWS) variations estimated from the data that GRACE minus GLDAS/Noah model and monthly groundwater level changes observed by monitoring wells during 2002-2012 (Table 2 in revised manuscript). Besides, according to the good comments of the Referee #2, we have compared the depletion in TWS or GWS between our results and previous studied results (e.g., Huang et al., 2015; Feng et al., 2013; Moiwo et al., 2013; Tang et al., 2013; Su et al., 2011) in the NCP (Table 2 in revised manuscript). The details of compare groundwater storage (GWS) variations with in-situ measurements and previous results, please see Section 4.1 in revised manuscript, we believe these discussions can validate GWS loss in NCP.

2) In part 5.2, GPS trend changes of water storage are different in two periods (2004-2009 and 2010- 2013), especially the long-term trend rate is different in different areas from 2010 to 2013. Are there any field measurement data of groundwater levels or groundwater use in different areas can support this result? In my opinion, the manuscript would be more improved if some groundwater data can be combined into this research.

> *Linsong Wang et al.:* Thank you again. As shown in Figure 8b in our study, the obvious uplifts are presented in the decomposition of the signal based on the

GRACE-derived GWS trend (GRACE minus GLDAS/Noah), which shows the long-term groundwater depletion in the NCP from 2002 to 2012. Recently, previous studies have reported the TWS loss (e.g., Zhong et al., 2009; Su et al., 2011; Moiwo et al., 2009) or GWS loss (e.g., Huang et al., 2015; Feng et al., 2013; Tang et al., 2013;) based on GRACE and land surface models (LSMs) in the NCP, these results are also consistent with that from in situ measurement data of groundwater levels. However, the water mass loss trend from GRACE and situ data show an inconsistency with the GPS results in our study, which you mentioned GPS trend changes of water storage are different in two periods (2004-2009 and 2010- 2013), especially the long-term trend rate is different in different areas from 2010 to 2013. For the reasons why the long-term trend rate from GPS is different in different areas, please see our detailed responses below.

1) The GPS is nowadays widely used in the geosciences for the estimation of precise station coordinates. The placement of a load on the Earth's surface causes deformation of the underlying solid Earth and displacements of its surface. GPS measurements of those displacements can provide information about the load.

2) Some previous studies have focused on the vertical component of crustal motion. These researches rely on the accurate interpretation of GPS motion in terms of surface stress or tectonic movement, and the deformation signal from surface mass loading is a source of noise. For these applications, they would like to obtain reliable

loading models or even surface mass observations, which can be used to reduce the contributions made to the GPS observations by the environmental loading. For some surface loads, such as the atmosphere, the loads are currently modeled to a fairly high degree of accuracy (van Dam et al., 1994). However, for other loads, especially the distribution of water mass on continents (soil moisture, groundwater, snow and ice), which are poorly known in most regions of the globe, but the deformation it causes is large enough to contribute to the GPS signal (van Dam et al., 2001). Fortunately, with the development of GRACE, the mass variations from hydrologic loading now can be quantitatively estimated. The GRACE-derived time-variable gravity field coefficients can be converted to harmonic coefficients for crustal deformation in three components.

3) In fact, it is more important to apply loading theory in the NCP. The previous studied results shown the groundwater depletion occurs in the shallow unconfined aquifers in Piedmont Plain while groundwater depletion occurs in the deep confined aquifers in the central and eastern plain of NCP. In this study, we found that GRACE-derived GWS changes are in disagreement with the groundwater level changes from observations of shallow aquifers not only from 2003 to 2009, especially from 2010 to 2013. Although the shallow groundwater can be recharged from the annual climate-driven rainfall (e.g., the groundwater level changes from observations of shallow aquifers shows a persistent increase after 2010, when the annual precipitation begins to increase), but the important facts indicate that GWS depletion

is more serious in deep aquifers. Especially in the central and eastern plain of NCP, although some GPS can detect land subsidence due to the occurrence of groundwater depletion in the deep confined aquifers, but the loading uplift effect from mass loss is still remain in GPS long-term trend. Thus, we compute the GRACE-derived long-term uplift using the trend from the CSR solutions for all continuous GPS sites used in this paper. The results indicate GRACE-derived data have an overall uplift in the whole region at the 0.37~0.95 mm/yr level from 2004 to 2009, but the rate of change direction is inconsistent in different GPS stations at -0.40~0.51 mm/yr level from 2010 to 2013 (Table 1). Our study indicates that the elastic responses are induced by all depth of TWS loading. Then we remove this hydrological-induced long-term trend from GPS actual observed vertical rates to derive the corrected vertical velocities (Figure 10), which can be used to study the vertical crust movement caused by tectonic movement and human activities. The results show that there are uplift areas and subsidence areas in NCP. Almost the whole central and eastern region of NCP suffers serious ground subsidence, caused by the anthropogenic-induced groundwater exploitation in the deep confined aquifers. In addition, that the ground uplifts lightly in the western region of NCP is mainly controlled by tectonic movement (e.g., Moho uplifting or mantle upwelling). Here Stokes coefficients resulted from A et al. [2013] were used to remove contributions from GIA.

Anonymous Referee #2 (Received and published: 13 December 2016)

General Comments:

This manuscript investigated the seasonal displacements of surface loadings in the NCP area using GRACE and GPS. The consistency between GPS and GRACE was quantitatively evaluated by removing GRACE-derived seasonal displacement from GPS observed detrended height time series. The rate of GRACE-derived TWS loss in the NCP was estimated and the land subsidence in the central and eastern of NCP was discussed. Generally the topic of manuscript is interesting and the writing is clear. However, in my opinion there are several important issues need to be addressed before publication.

Dear Anonymous Referee #2,

Thanks very much for your constructive comments. We have studied comments carefully and here replied each comment bellow. The original comments are in plain text and the replies in italics which we hope meet with approval.

Major points:

1. Recently lots of publications regarded on the estimation of TWS variation in the NCP, such as Huang et al. (2015), Feng et al. (2013), Moiwo et al. (2013), Tang et al. (2013) (listed in the manuscript) and some other references (e.g. Su et al., 2011). These studies should be included in the discussion to compare the depletion in TWS in the NCP.

>Linsong Wang et al.: Thank you very much for the good comments that you mentioned previous studies should be included in the discussion. In revised manuscript, we have compared the depletion in TWS or GWS between our results and previous studied results (i.e., add comparisons to the Table 2 including mass loss trend from our results and previous studied in the revised manuscript) in the NCP, e.g., the reported TWS loss from Zhong et al.(2009), Su et al.(2011), Moiwo et al.(2009), and the reported GWS loss from Huang et al.(2015), Feng et al.(2013), Tang et al.(2013). Besides, according to the good comments of the Referee #1, we have also compared the groundwater depletion in NCP between GWS variations estimated from the data that GRACE minus GLDAS/Noah model and monthly groundwater level changes observed by monitoring wells during 2002-2012 (Table 2 in revised manuscript), we believe these discussions can validate GWS loss in NCP.

2. Results and discussion should be presented separately, since some result sections (e.g. section 3) include discussion parts (e.g. lines 308-326, lines 356-359). I would suggest moving the relevant parts to section 5 for discussion.

>Linsong Wang et al.: Thanks for your good suggestion. In revised manuscript, we have moved the discussion parts of section 5.1 “Groundwater Depletion Contributions to Long-Term Uplift” in original manuscript to the section 4.2, which is mainly to explain long-term uplift caused by TWS loss, especially the contributions from groundwater depletion in the NCP. Then, we have added new discussion in Section 5.1 “The Loading Effects of Non-tidal Ocean and Atmospheric Variations”

for discussing the cause of the difference between our results and previous studies, which you mentioned “some result sections (e.g. section 3) include discussion parts (e.g. lines 308-326, lines 356-359)”.

3. There are some grammatical errors in the paper, meanwhile some sentences are not well written (e.g., lines 301-302, lines 335-338, lines 422-424, line 448). Please check it carefully throughout the manuscript.

>Linsong Wang et al.: Thank you again. We rewrote your mentioned some sentences (please see lines 317-319, lines 332-337, lines 491-497 in revised manuscript) and the revised version of the manuscript was polished by one language editor (please see the Marked manuscript).

Specific Comments:

1. Page 1, line 15: please remove “We employ” from the sentence.

>Linsong Wang et al.: Thank you. We have removed “We employ” from the sentence in the revised manuscript.

2. Page 1, lines 17 and 19: please give the full name of “NCP” and “WRMS”, since it first appeared in the paper.

>Linsong Wang et al.: Thank you. We have given the full name of “NCP” and “WRMS” where they first appear in the paper.

3. Line 367: should be “equations (2) and (3)”.

>*Linsong Wang et al.: Thank you for reminding our negligence. The mistake has been modified.*

4. Line 369: » “was presented: : :”

>*Linsong Wang et al.: Thank you. “were presented” has been changed to “was presented” in the revised manuscript.*

5. Line 388: » “under- or overestimation: : :”

>*Linsong Wang et al.: Thank you. “under or overestimation” has been revised to “under- or overestimation” in the revised manuscript.*

6. Line 449: » “before and after removing: : :”

>*Linsong Wang et al.: Thank you. “before and after remove” has been changed to “before and after removing” in the revised manuscript.*

7. Line 488: “two periods” » “two sub-periods”

>*Linsong Wang et al.: Thank you. “two periods” has been changed to “two sub-periods” in the revised manuscript.*

References:

Su, X. L., J. S. Ping, and Q. X. Ye (2011), Terrestrial water variations in the North China Plain revealed by the GRACE mission, *Sci. China Earth Sci.*, 54 (12), 1965–1970, doi:10.1007/s11430-011-4280-4.

>*Linsong Wang et al.: Thank you for providing the reference of previous studies.*

We tried our best to improve the manuscript and made some changes in the manuscript. These changes will not influence the content and framework of the paper. And here we did not list the changes but marked in the "The marked-up manuscript version ".

We appreciate Editors/Reviewers' warm work earnestly, and hope that the correction will meet with approval.

Once again, thank you very much for your comments and suggestions.

Linsong Wang et al.

Part II . The marked-up manuscript version

The revision mainly includes:

1. Rewrote abstract basing on revised content;
2. A Large adjustment of the structure in section 3, 4 and 5;
3. In-situ groundwater level measurements and previous studied results in NCP are added and analyzed (Figure 7 and Table 2);
4. More discussion has been put on validation of the results.
5. Rewrote not well sentences and language improvement;
6. Update the supporting information.

1 **The marked manuscript:**

2
3 **Detecting seasonal and long-term vertical displacement in the North**
4 **China Plain using GRACE and GPS**

5
6 Linsong Wang^{1,2}, Chao Chen^{1,2}, Jinsong Du¹, and Tongqing Wang³

7 ¹Hubei Subsurface Multi-scale Imaging ~~Key Laboratory Lab (SMIL)~~, Institute of Geophysics and
8 Geomatics, China University of Geosciences, Wuhan, Hubei, China

9 ²Three Gorges Research Center for Geo-hazard, Ministry of Education, China University of
10 Geosciences, Wuhan, Hubei, China

11 ³First Crust Deformation Monitoring and Administration Center, China Earthquake Administration,
12 Tianjin, China

13
14 * Corresponding author: Linsong Wang, wanglinsong@cug.edu.cn

15
16 **Abstract:**

17 ~~Twenty~~We employ ~~twenty~~nine continuous Global Positioning System (GPS) time series data
18 together with data from Gravity Recovery and Climate Experiment (GRACE) are analyzed to
19 determine the seasonal displacements of surface loadings in the ~~North China Plain (NCP)~~.
20 Results show significant seasonal variations and a strong correlation between GPS and
21 GRACE results in the vertical displacement component; the average correlation and ~~Weighted~~
22 ~~Root-Mean-Squares (WRMS)~~ reduction between GPS and GRACE are 75.6% and 28.9%~~%~~.

23 respectively, when atmospheric and non-tidal ocean effects were removed, but the ~~peak-to~~
24 ~~peak~~ annual peak-to-peak amplitude of GPS (1.2~6.3 mm) is greater than the data
25 ~~GRACE-derived~~ (1.0~2.2 mm) derived from GRACE. We also calculate the trend rate as
26 well as the seasonal signal caused by the mass load change from GRACE data, the rate of
27 GRACE-derived Terrestrial Water Storage (TWS) loss (after multiplying by the scaling factor)
28 in the NCP was 3.39 cm/yr (equivalent to 12.42 km³/yr) from 2003 to 2009. For a 10-year
29 time span (2003 to 2012), the rate loss of TWS was 2.57 cm/yr (equivalent to 9.41 km³/yr)
30 which is consistent with the groundwater storage (GWS) depletion rate (the rates loss of GWS
31 were 2.49 cm/yr and 2.72 cm/yr during 2003~2009 and was 2.57 cm/yr (equivalent to 9.41
32 km³/yr) 2003~2012, respectively) estimated from GRACE-derived results after removing
33 simulated soil moisture (SM) data from GLDAS/Noah model. We also found that
34 GRACE-derived GWS changes are in disagreement with the groundwater level changes from
35 observations of shallow aquifers from 2003 to 2009, especially between 2010 and 2013.
36 Although the shallow groundwater can be recharged from the annual climate-driven rainfall
37 (e.g., the groundwater level changes from observations of shallow aquifers show a persistent
38 increase after 2010 when the annual precipitation begins to increase), but the important facts
39 indicate that GWS depletion is more serious in deep aquifers. Basing on spherical harmonic
40 coefficients for the gravity field and load Love numbers, we use GRACE model to remove the
41 vertical rates of elastic displacements due to the surface mass ~~changes~~change from GPS data.
42 The GRACE-derived result shows an overall uplift ~~infor~~ the whole region at the
43 0.37~0.95 ~~04~1.47~~ mm/yr level from 2004 to 2009, but the rate of change direction is
44 inconsistent in different GPS stations at -0.40~-0.51 mm/yr level from 2010 to 2013. Then we

45 ~~removed the uplifted vertical rates which are induced by TWS from GPS-derived data to~~
46 ~~obtain the corrected vertical velocities caused by tectonic movement and human activities.~~
47 ~~The results show that there are uplift areas and subsidence areas in NCP. Almost the whole~~
48 ~~central and eastern region of NCP suffers serious ground subsidence caused by the~~
49 ~~anthropogenic-induced groundwater exploitation in the deep confined aquifers. In addition,~~
50 ~~the slight ground uplifts in the western region of NCP are mainly controlled by tectonic~~
51 ~~movement (e.g., Moho uplifting or mantle upwelling).-0.94-2.55 mm/yr level from 2010 to~~
52 ~~2013.-~~

53
54 **Keywords:** GPS, GRACE, Seasonal and long-term displacement, Terrestrial water storage,
55 the North China Plain

57 **1. Introduction**

58 Using Global Positioning System (GPS) to monitor crustal motion, especially in the vertical
59 or height component due to its large amplitude, which has been used to study surface loading
60 caused by mass change. Site-position time series recorded by continuous GPS arrays have
61 revealed ~~the that~~ vertical displacement variations ~~resulted~~~~ean result~~ from trend or seasonal
62 distribution of mass in a region or global changes ~~that cause displacement of the Earth's~~
63 ~~surface~~ (e.g., a change of continental water [Bevis et al., 2005; van Dam et al., 2007; Wahr et
64 al., 2013], ice [Sauber et al., 2000; Khan et al., 2010; Nielsen et al., 2013], snow [Heki, 2001;
65 Grapenthin et al., 2006], ocean [van Dam et al., 2012; Wahr et al., 2014] and atmospheric
66 mass [van Dam et al., 1994; Boehm et al., 2007]).

67

68 On the global scale, terrestrial hydrologic mass exchanges; that causes significant large-scale
69 loading; occur between the oceans, continents, and atmosphere at seasonal and inter-annual
70 time scales. On the local scale, for the inter-annual and long-periodic change in the hydrologic
71 cycle, ~~what-that-most~~ significantly affects loading are large anthropogenic disturbances on
72 groundwater extraction and artificial reservoir water impoundment and other climate-driven
73 factors (e.g., natural floods and droughts) [e.g., Chao et al., 2008; Rodell et al., 2009; Feng et
74 al., 2013; Joodaki et al., 2014; Wang et al., 2014]. The global-scale mass variations closely
75 related to changes in terrestrial water storage (TWS) are observed by the Gravity Recovery
76 and Climate Experiment (GRACE) satellite mission, while the surface elastic displacement
77 can be estimated if the load and rheological properties of the Earth were known [Farrell,
78 1972]. The majority of previous loading studies solved the three components of crustal
79 motion by adopting joint analysis of GRACE time-variable gravity field coefficients and GPS
80 data [Kusche and Schrama, 2005; van Dam et al., 2007; Fu and Freymueller, 2012; Fu et al.,
81 2013]. In principle the loading effects caused by the majority of mass redistributions near the
82 Earth's surface are from water, atmospheric, and ocean transports on daily to inter-annual
83 timescales [Kusche and Schrama, 2005]. ~~The The variations of the atmospheric and ocean~~
84 contribution to the surface displacement made by the variations of the atmospheric and ocean
85 can be reasonably modeled ~~by, and therefore corrected,~~ using global atmospheric surface
86 pressure data and space geodetic data; respectively. Thus, after removing the loading effects
87 of the atmospheric and ocean, GRACE-derived displacement and GPS data allow the
88 detection of changes in the Earth's larger hydrological storage systems.

89

90 In general, changes in TWS capacities depend on precipitation and human consumption.

91 Variations in TWS may be related to precipitation, which is strongly driven by climate and

92 can be simulated from global water and energy balance models [Syed et al., 2008]. This is

93 related to soil texture and root depth in the case of soil water storage (e.g., soil moisture and

94 vegetation canopy storage can be derived from the Global Land Data Assimilation System

95 (GLDAS) [Rodell et al., 2004], the WaterGAP Global Hydrology Model (WGHM) [Döll et al.,

96 2003] and the Community Land Model (CLM) [Oleson et al., 2013]), surface water storage

97 (e.g., water in rivers, lakes, reservoirs and wetlands can be derived from WGHM while snow

98 or ice can be derived from WGHM and CLM), and naturally occurring (i.e., climate-driven)

99 aquifer storage (e.g., groundwater predicted by WGHM and CLM). Variations in TWS may

100 also be caused by man-made factors, such as water withdrawals for irrigation purposes [Döll,

101 2009] and dam construction for power generation and navigation [Wang et al., 2011]. These

102 changes in TWS can be observed in situ (i.e., groundwater level and impounded water level).

103 ~~The TWS integrated by all the~~The TWS integrated by all the~~All can cause~~ variations ~~in TWS~~ can lead to the overall changes

104 in crust displacement.

105

106 This study focuses on the crustal deformation of the North China Plain (NCP) (Figure 1),

107 which is one of the most uniformly and extensively altered areas by human activities in the

108 world [Tang et al., 2013]. The NCP is one of the world's largest aquifer systems and supports

109 an enormous exploitation of groundwater. Overexploitation of groundwater has seriously

110 affected agriculture irrigation, industry, public supply, and ecosystems in the NCP. Previous

111 studies used GRACE data, land surface models, and well observations to provide insight on
112 groundwater depletion in the NCP [Su et al., 2009; Zhong et al., 2009; Feng et al., 2013;
113 Moiwo et al., 2013; Tang et al., 2013; Huang et al., 2015]. Liu et al. [2014] has discussed
114 loading displacement in the NCP before. Only five GPS stations (i.e., BJFS, BJSH, JIXN,
115 TAIN, and ZHNZ) data are used in their work. Although they calculated the seasonal
116 amplitudes, phases and trends of vertical displacement from GRACE and GPS, the
117 atmospheric and non-tidal ocean loading effects were not removed in the Liu et al.'s work, i.e.,
118 they added the Atmosphere and Ocean De-aliasing Level-1B (AOD1B) solution (GAC
119 solution) back to the GRACE spherical harmonic solutions.

120

121 Here, we use GRACE and data from 29 GPS sites to study the seasonal and long-term loading
122 displacement due to dynamic hydrological processes and groundwater-derived land
123 subsidence in the NCP. In contrast to previous focus study [Liu et al., 2014], the most
124 obvious difference between our results and their work is we removed other loading effects
125 (e.g., atmospheric and non-tidal ocean) in order to reflect the seasonal and long-term
126 displacement caused by TWS loads better. Additionally, we discuss long-term trend due to
127 mass change revealed by GRACE measurements and its impacts on tectonic vertical rates
128 evaluations.

129

130 **2. Data Analysis**

131 **2.1 GRACE Data**

132 The GRACE mission design makes it particularly useful for time-variable gravity studies.

133 GRACE was jointly launched by NASA and the German Aerospace Center (DLR) in March
134 2002 [Tapley et al., 2004a]. The Level-2 gravity products consist of sets of complete ~~sets of~~
135 spherical harmonic (Stokes) coefficients out to some maximum degree and order (typically
136 $l_{max} = 120$) averaged over monthly intervals. When considering large-scale mass redistribution
137 in the Earth system on a timescale ranging from weekly to interdecadal, it is reasonable to
138 assume that all relevant processes occur in a thin layer at the Earth's surface [Kusche and
139 Schrama, 2005]. In this analysis, we assume that the gravitational and geometrical response of
140 the Earth can be described by Farrell's [1972] theory, where the loads Love numbers only
141 depend on the spherical harmonic degree. Thus, the elastic displacements due to the surface
142 mass change can easily be represented in terms of spherical harmonic coefficients for the
143 gravity field and load Love numbers, k_l , l_l , and h_l [Wahr et al., 1998; Kusche and Schrama,
144 2005]. Level-2 products are generated at several project-related processing centers, such as
145 the Center for Space Research (CSR) at the University of Texas, GeoForschungsZentrum
146 (CSR) in Potsdam, Germany, and the Jet Propulsion Laboratory (JPL) in California. The mass
147 estimates (TWS and sea level) show very good agreement among these products [Fu and
148 Freymueller, 2012; Wahr et al., 2014; Wang et al., 2014].

149

150 This study used monthly sets of spherical harmonic (Stokes) coefficients from GRACE RL05
151 (i.e., Release 5) gravity field solutions generated from the CSR, spanning from February 2003
152 to April 2013. Each monthly GRACE field consisted of a set of Stokes coefficients, C_{lm} and
153 S_{lm} , up to a degree and order (l and m) of 60. In fact, the GRACE Stokes coefficients ("GSM"
154 coefficients denoted by the GRACE Project) have had modeled estimates of the atmospheric

155 and oceanic mass signals removed. Thus the GRACE coefficients include the full terrestrial
156 water storage signal with remaining atmospheric and oceanic signals due to errors in the
157 respective models [Swenson et al., 2008]. Generally, using the GRACE AOD1B products can
158 add back the de-aliasing atmospheric and non-tidal oceanic effects to the GRACE data.
159 However, we would like to reduce the environmental loading contributions to the GRACE
160 and GPS observations, if we study on the accurate interpretation of displacement due to TWS
161 loading. Thus, we analyzed ~~on~~ the effects of non-tidal ocean variations and atmospheric
162 loading on the GRACE model and GPS coordinates, please see Section S1 in the supporting
163 information for details.

164

165 We replaced the GRACE C_{20} coefficients with C_{20} coefficients inferred from satellite laser
166 ranging [Cheng et al., 2013]. Due to the fact that the reference frame origin used in the
167 GRACE gravity field determination is the Earth's center of mass (CM), GRACE cannot
168 determine the degree-1 terms variations in the Earth's gravity field (geocenter motion). Here,
169 we used degree-1 coefficients as calculated by Swenson et al. [2008] to determine the position
170 of the CM relative to the center of figure (CF) of the Earth's outer surface. We applied the
171 post-processing method described in Swenson and Wahr [2006] to remove north-south stripes.
172 We adopted 250 km as the averaging radius to implement Gaussian smoothing, a technique
173 which suppresses errors at high degrees [Wahr et al., 1998; van Dam et al., 2007]. Stokes
174 coefficients ~~resulted~~ results from A et al. [2013] were used to remove contributions from
175 Glacial Isostatic Adjustment (GIA). The contribution of GIA is about 0.28 ~~–~~ 0.33 mm/yr and
176 non-seasonal in the NCP, which is small and non-seasonal; so their impact on the seasonal

177 results discussed in this paper would be minimal, even if they were not removed.

178 The spatial pattern of TWS, shown in Figure 2, was obtained from monthly GRACE mass
179 solutions for NCP and surrounding regions between spring, 2003, and spring, 2013. An
180 obvious negative trend was identified localized over North China, including some of the
181 Northwest regions (i.e., Shanxi province) and Northeast regions (i.e., Liaoning province). The
182 TWS changes derived from the GRACE data show significant loss trends across the entire
183 study area (NCP), specifically in Beijing, Tianjin, Hebei province, and Shanxi province.
184 Previous studies have investigated how much groundwater depletion has caused the
185 GRACE-derived TWS loss in the whole of the NCP [[Su et al., 2009](#); Feng et al., 2013; Moiwo
186 et al., 2013] or in different sub-regions of the NCP [[Zhong et al., 2009](#); Tang et al., 2013;
187 Huang et al., 2015]. These investigations, however, did not focus on regional displacement
188 due to seasonal or long term variations of hydrologic loading.

189

190 **2.2 GPS Data**

191 Twenty-four GPS sites from the Crustal Movement Observation Network of China
192 (CMONOC) and five GPS sites from the International GNSS Service (IGS) (Table 1) were
193 analyzed in this study (Figure 1 shows the locations of the GPS stations). Eight GPS sites of
194 them were located in the surrounding area of the NCP. Daily values for the upward, eastward
195 and northward coordinates were determined by GPS data of IGS stations between 2003 and
196 2013, which is consistent with GRACE time span. The 24 GPS sites of CMONOC provided
197 data from 2010 to 2013. GIPSY/OASIS-II (Version 5.0) software was used in point
198 positioning mode to obtain the daily coordinates and covariances; these were used to

199 transform the daily values into ITRF2008 [Altamimi et al., 2011]. We estimated this daily
200 frame alignment transformation using a set of reliable ITRF stations (~10 stations each day).
201 In the GPS processing, corrections for solid Earth tides were undertaken, and ocean tide
202 loading effects were corrected using ocean tide model FES2004 with Greens Functions
203 modeled in the reference frame of CM (center of the mass of the total Earth system) to
204 maintain theoretical consistency and adherence to current IERS conventions [Hao et al., 2016;
205 Fu et al., 2012], but atmospheric pressure loading or any other loading variations (non-tidal
206 ocean loading) with periods > 1 day were not removed. In order to focus on the seasonal and
207 trend feature over the entire observation time, we first smoothed the data to reduce large
208 scatter before using a 3-month-wide moving window filter to remove the short-period terms.

209

210 Due to the coseismic displacement of the 2011 Mw9.0 Tohoku earthquake, we estimated and
211 removed offsets (i.e., using the differences of the average values of seven days between
212 before and after earthquake to obtain the coseismic displacement) at those times for the
213 vertical time series of GPS stations at Eastern China. Wang et al. [2011] study results reveal
214 that the coseismic horizontal displacements induced by the earthquake are at the level of
215 millimeters to centimeters in North and Northeast China, with a maximum of 35 mm, but the
216 vertical coseismic and postseismic displacements are too small to be detected. In order to
217 maintain consistency with the GIA effects ~~presented~~present in the GRACE solutions, we
218 remove GIA effects for all GPS stations by using Stokes coefficients ($l=100$) results computed
219 by A et al. [2013], which used the ICE5G ice history and VM2 viscosity profile [Peltier et al.,
220 2004].

221

222 | Figure 3a shows the time series (2003–2012) of daily solutions for IGS GPS sites BJFS,
223 ZHNZ, BJSH, JIXN and TAIN. The long-term linear trends are mainly dominated by surface
224 mass loading and tectonic processes, and the GPS time series shows significant seasonal
225 variations. The peak-to-peak seasonal amplitude can be seen to be more than 20 mm which
226 reflects the strong seasonal mass changes in the NCP. The GRACE data from CSR uses model
227 output to remove the gravitational effects of atmospheric and oceanic mass variability from
228 the satellite data before constructing monthly gravity field solutions. In order to compare the
229 displacement from GPS with GRACE, the effects of atmospheric and non-tidal oceanic
230 loading on the GPS coordinates needed to be removed. Displacements due to atmospheric
231 loading were calculated using data and programs developed by the GGFC (Global
232 Geophysical Fluid Center) (T. van Dam, NCEP Derived 6 hourly, global surface
233 displacements at $2.5^\circ \times 2.5^\circ$ spacing, <http://geophy.uni.lu/ncep-loading.html>, 2010). These
234 utilized the NCEP (National Center of Environmental Protection) reanalysis surface pressure
235 data set. The 12-hour sampling model, ECCO (Estimating the Circulation & Climate of the
236 Ocean, <http://www.ecco-group.org/>), is used to compute the surface displacement driven by
237 non-tidal ocean effects and its spatial resolution is $1^\circ \times 0.3-1.0^\circ$; i.e., 1 degree longitude (zonal)
238 interval and 0.3 to 1.0 degree in latitude (meridian) intervals from equator to high latitude. An
239 example of the effects of the non-tidal ocean and atmospheric loading in the GPS and
240 GRACE data is provided in the supporting information (Figure S1).

241

242 The displacements caused by atmospheric pressure and non-tidal ocean loading mainly show

243 seasonal fluctuations and no obvious long-term trend during GPS observation (e.g., time
 244 series of height from atmospheric and non-tidal ocean loading at IGS sites in Figure 3b). The
 245 annual amplitude is 4.0~4.6 mm and 0.24~0.42 mm for the atmospheric and non-tidal
 246 ocean loading effects, respectively, while the semi-annual amplitude is about 0.3 mm and 0.03
 247 mm, respectively. But the phases between the atmospheric and non-tidal ocean loading effects
 248 have more apparent difference. The results of the seasonal amplitudes and phase fits of
 249 vertical displacements, derived by GRACE and GPS for IGS stations between before and
 250 after ~~correcting~~ corrected atmospheric and non-tidal ocean, are summarized in Table S1 in the
 251 supporting information.

252

253 2.3 Elastic Displacements Due to Mass Loads

254 GRACE Stokes coefficients [Wahr et al., 1998] and load Love numbers [Farrell, 1972] can be
 255 used to estimate the displacement effects in three components (Up, North and East) caused by
 256 mass load changes. The mathematical relationships [Kusche and Schrama, 2005; van Dam et
 257 al., 2007] between the radial surface displacement (Up or Height) and the Stokes coefficients
 258 of mass is:

$$259 \quad \Delta h = dr(\theta, \phi) = R \sum_{l=1}^{N_{max}} \sum_{m=0}^l \tilde{P}_{l,m}(\cos \theta) \cdot (C_{lm} \cos(m\phi) + S_{lm} \sin(m\phi)) \frac{h_l}{1 + k_l} \quad (1)$$

260 where Δh is the displacement of the Earth's surface in the radial direction at latitude θ (theta)
 261 and eastward longitude ϕ (phi); $N_{max}=60$, R is the Earth's radius; $\tilde{P}_{l,m}$ is fully normalized
 262 Legendre functions for degree l and order m ; C_{lm} and S_{lm} are time variable components of the
 263 (l,m) Stokes coefficients for some month; and h_l , k_l and l_l are the three degree dependent load
 264 Love numbers which are functions of Earth's elastic property. In this equation we adopted the

265 load Love numbers provided by Han and Wahr [1995].

266

267 Similarly, horizontal displacements (North and East) can be calculated using the following
268 equations:

$$269 \quad \Delta n = dr(\theta, \phi) = -R \sum_{l=1}^{N_{\max}} \sum_{m=0}^l \frac{\partial}{\partial \theta} \tilde{P}_{l,m}(\cos \theta) \cdot (C_{lm} \cos(m\phi) + S_{lm} \sin(m\phi)) \frac{l_l}{1+k_l}, \quad (2)$$

$$270 \quad \Delta e = dr(\theta, \phi) = \frac{R}{\sin \theta} \sum_{l=1}^{N_{\max}} \sum_{m=0}^l \tilde{P}_{l,m}(\cos \theta) \cdot m(-C_{lm} \sin(m\phi) + S_{lm} \cos(m\phi)) \frac{l_l}{1+k_l}, \quad (3)$$

271 where Δn and Δe are north and east components of the displacement, respectively, ~~with~~ both
272 having positive values when the crust moves towards the north and east, respectively. As is
273 mentioned in Section 2.1 above, in order to be consistently comparable to the GPS time series,
274 we corrected the degree-1 components to GRACE-derived mass variations, using Stokes
275 coefficients derived by Swenson et al. [2008]. With corresponding to degree-1 contribution to
276 vertical displacement, the value of load Love numbers of the degree-1 in the CF frame should
277 be computed by using equation (23) in Blewitt [2003].

278

279 Figure 4 shows an example (site BJFS, JIXN, TAIN and ZHNZ) of the GRACE-derived
280 vertical (Figure 4c) and horizontal displacements (Figure 4a and 4b) before and after
281 destriping. It can be clearly ~~be~~ seen that the maximal amplitude of vertical displacement is
282 several order of magnitude higher than horizontal displacements. In addition, the calculated
283 results using the monthly GRACE model data after destriping show that the effects of TWS
284 (soil moisture, etc.) on surface displacements are seasonal variations and long-term changes
285 on vertical and horizontal components. As most of the stations are located in areas of TWS

286 loss in the NCP (see sites location in Figure 2), the fact is that the motion is upward (see the
287 positive trend of GRACE-derived vertical in Table 1) during this event (if a load is removed,
288 the site uplifts and moves away from the load [Wahr et al., 2013]). Identified horizontal
289 displacements are important as they constrain the location of load changes [Wahr et al., 2013;
290 Wang et al., 2014]. The displacement of the ZHNZ site is upwards and to the south (see the
291 negative trend of the ZHNZ north component in Figure 4a) due to the mass loss almost due
292 north of the site. Correspondingly, the displacement of the TAIN site is upwards and to the
293 southeast (see the negative trend of the north component and the positive trend of the east
294 component of the TAIN site in Figure 4a and 4b) caused by the mass loss located to the
295 northwest of the site, based on the use of GPS horizontals for loading studies from Wahr et al.
296 [2013].

297

298 **3. GRACE-derived Seasonal Variations and Comparison with GPS Measurements**

299 Using equation (1) and GRACE-derived Stokes coefficients, the vertical displacements at the
300 GPS sites in the NCP and its surrounding region can be calculated. To focus on these changes,
301 GRACE-derived vertical displacements were computed by fitting a model with a linear trend
302 and annual periodic terms using Least-Squares method over the entire 11 year time span, for a
303 comparison to the seasonal variations observed by GPS (Table 1). Figure 5 shows time series
304 of vertical displacements for GPS sites of IGS stations (BJFS, BJSH, JIXN, TAIN and ZHNZ).
305 The fitting results show the GRACE-derived (without ADO1B) peak-to-peak annual
306 amplitudes can be more than 2 mm, and the semi-annual amplitude are also visible at these
307 five GPS sites. This reflects the climate-derived seasonal hydrological fluctuations in the

308 NCP.

309

310 Compared with GRACE results mainly due to the mass change in seasonal and long-term
311 linear period, all GPS time series show significant seasonal and long-term trends which are
312 mainly dominated by tectonic and hydrological process. The fitting results (after
313 Least-Squares fitting) show the peak-to-peak vertical seasonal displacements from GPS time
314 series are to be larger than GRACE-derived results at those GPS sites, and the peak-to-peak
315 seasonal amplitude changes between 5 mm and 6 mm (Table 1). The results of the comparison
316 between GPS and GRACE-derived seasonal height variations at 24 GPS sites from
317 CMONOC can be seen in Figure S3 in the supporting information. For all the selected GPS
318 sites, the annual component is more dominant than the semi-annual one. The peak-to-peak
319 annual amplitude is 1.2~6.3 mm and 1.0~2.2 mm for the GPS and GRACE solutions,
320 respectively, while the semi-annual amplitude is about 1/2~1/3 times of that in annual
321 amplitude. These more consistent seasonal variations of GRACE and GPS height time series
322 reflect the climate-derived seasonal hydrologic process, i.e., heavy monsoonal precipitation in
323 the late summer months result in mass loads increase (the maximum negative of vertical
324 amplitude) and largely ~~pumping~~~~pumped~~ for agricultural usage in late spring months cause
325 mass loads decrease (the maximum positive of vertical amplitude). The facts show~~We observe~~
326 ~~the fact that the amplitude of GPS data is relatively has a larger amplitude than that of~~
327 ~~GRACE-derived displacements, which does, it is not merely exist~~~~only exists~~ in the IGS
328 ~~stations, but also in almost all CMONOC stations except SXGX (Table 1).~~ This indicates that
329 GPS has a strong sensitivity for local surface loading. By contrast, because the spatial

带格式的: 字体颜色: 红色

带格式的: 字体颜色: 红色

带格式的: 字体颜色: 红色

带格式的: 字体颜色: 红色

带格式的: 字体颜色: 红色

带格式的: 字体颜色: 红色

带格式的: 字体颜色: 红色

带格式的: 字体颜色: 红色

带格式的: 字体颜色: 红色

带格式的: 字体颜色: 红色

带格式的: 字体颜色: 红色

330 resolution of GRACE data is limited to approximately 300 km ($N_{max}=60$), GRACE-derived
331 results are mainly constrained by large scale areas. This means that GRACE-derived vertical
332 displacements show a small difference between stations due to the results are averaged over
333 scales of several hundred km or more.

334

335 ~~As is mentioned above, the cause of the difference between our results and Liu's work [Liu et~~
336 ~~al., 2014] is we removed atmospheric and non-tidal ocean loading effects while they did not.~~
337 ~~However, we found that the amplitude of GPS after removed atmospheric and non-tidal ocean~~
338 ~~loading effects, is still greater than the GRACE while we added the AOD1B de-aliasing~~
339 ~~model to the GRACE solutions (i.e., no atmospheric and non-tidal ocean corrected, please see~~
340 ~~the Table S1 in the supporting information). The most obvious difference between our results~~
341 ~~and Liu's work [Liu et al., 2014] is that they adopt the load Love numbers from Guo et al.~~
342 ~~[2004] to transform these coefficients into vertical surface displacement estimates. We check~~
343 ~~the two results of Love numbers (ocean load and atmospheric pressure load) from Guo et al.~~
344 ~~[2004], there are significant differences between ocean load and atmospheric pressure load~~
345 ~~Love numbers. Meanwhile, we compared k_n Love numbers from Guo et al. [2004] (Liu et al.'s~~
346 ~~work) and k_n Love numbers from Han and Wahr [1995] (our work) with the k_n Love numbers~~
347 ~~used in AOD1B products [Farrell, 1972], respectively. The different Love numbers have~~
348 ~~caused the amplitude of the same station from Liu's GRACE derived vertical displacements~~
349 ~~much more than GPS and our GRACE results, due to k_n from atmospheric pressure load Love~~
350 ~~numbers [Guo et al., 2004] significantly larger than Love numbers from Han and Wahr [1995]~~
351 ~~and Farrell [1972]. The detailed analysis of the different Love numbers from Guo et al. [2004],~~

352 ~~Han and Wahr [1995] and Farrell [1972], please see the Section S1 in the supporting~~
353 ~~information~~

354

355 Next, we compare GPS observed and GRACE-derived seasonal height variations. The
356 estimated annual amplitudes and initial phases derived from GPS (grey vector) and GRACE
357 (red vector) are shown in Figure 6. We find that there are many sites where the signals
358 disagree in both amplitude and phase. The annual amplitudes and phases from
359 GRACE-derived results are much more spatially coherent than those determined from the
360 GPS heights ~~because~~. ~~Because~~ GRACE solutions truncate to $l_{max}=60$ and the Gaussian

361 filtering was used to lead to so smooth out concentrated loads. ~~The phase results~~ ~~phases~~ of the

362 ~~GRACE-derived displacements~~ ~~data~~ show that the annual signal peaks ~~basically~~

363 ~~appear~~ ~~(summer monsoon)~~ ~~basic~~ between September and October, which indicates a ~~and~~

364 ~~indicate that the~~ ~~maximum load occurs in this two months~~ ~~(summer monsoon)~~. ~~However~~. ~~But~~

365 there are several ~~differences between the results of GPS and GRACE in some sites, more~~

366 ~~specifically, where~~ the GRACE signals disagree in phase with GPS data, which the annual

367 ~~signal peaks~~ ~~sometimes appears~~ ~~sometime~~ between August and September according to GPS

368 ~~data~~. The five signals of sites in the northwest foothills region of NCP agree in phase, while

369 annual amplitudes from GRACE are significantly less than GPS, e.g., NMTK, NMZL, HEYY,

370 HEZJ and HECC. The cause of ~~most~~ ~~mostly~~ phase inconsistency may be the different spatial

371 resolution of GRACE compared to GPS. That is, GPS measurements can sense the difference

372 between loads very near the site, and loads a bit further away, but GRACE with wavelengths

373 on the order of 300 km reflects this variation at a monthly scale. Another important reason is

带格式的: 字体颜色: 红色

带格式的: 字体颜色: 红色

带格式的: 字体颜色: 红色

带格式的: 字体颜色: 红色

带格式的: 字体颜色: 红色

带格式的: 字体颜色: 红色

带格式的: 字体颜色: 红色

带格式的: 字体颜色: 红色

带格式的: 字体颜色: 红色

带格式的: 字体颜色: 红色

带格式的: 字体颜色: 红色

374 that a one-month sampling of GRACE means a phase sampling of 30° , while a one-day
375 sampling of GPS means a phase sampling of $\sim 1^\circ$, the different temporal sampling rate caused
376 the inconsistent phase between GRACE and GPS.

377

378 With the purpose of quantitatively evaluating the consistency between GPS and GRACE, we
379 remove GRACE-derived seasonal displacement from GPS observed detrended height time
380 series to compute the reductions of Weighted Root Mean Squares (WRMS) based on the
381 equation (2) in van Dam et al. [2007]. Correlation between GPS and GRACE derived
382 seasonal variations and WRMS reduction ratio of remove GRACE-derived seasonal
383 displacement from GPS observed detrended height time series, please see the Table ~~S3S4~~
384 the supporting information for details. All the selected sites show high correlation (~~85%~9%~~
385 99%, without TJBH site) when atmospheric and non-tidal ocean effects was not removed. ~~Our~~
386 ~~correlation results of IGS stations (BJFS, BJSH, JIXN, TAIN and ZHNZ) are consistent with~~
387 ~~Liu's work [Liu et al., 2014], indicating that the seasonal variations might come from the~~
388 ~~same geophysical process. The WRMS residual reduction ratio for all the stations ranged~~
389 ~~from 19% to 85%, which is better than Liu's work [Liu et al., 2014]. However, the correlation~~
390 ~~and WRMS reduction between GPS and GRACE are weak when atmospheric and non-tidal~~
391 ~~ocean effects was removed, with the average correlation and WRMS reduction reduce to 75.6%~~
392 ~~and 28.9%, respectively. This is mainly because the seasonal hydrologic process is major~~
393 ~~contributors to seasonal changes, and different stations are greatly influenced by the~~
394 ~~surrounding hydrological process.~~ By contrast, the seasonal amplitudes and phases from
395 GRACE results are much more spatially coherent than those determined from the GPS

396 heights, caused by the different spatial resolution between them. In addition, we also attempt
397 to calculate GRACE-derived horizontal displacement using ~~equation~~equation (2) and (3),
398 and compare it with the GPS measurements. An example (five IGS sites) of the comparison
399 between GRACE-derived and GPS observed horizontal displacements ~~was~~were presented to
400 demonstrate the correlation of seasonal horizontal variation caused by surface hydrological
401 load. Please see the Figure S4 in the supporting information.

402

403 **4. Long-Term Uplift Caused by TWS Loss**

404 **4.1 Compare Groundwater Storage (GWS) Variations With in-situ Measurements and**

405 **Previous Results**

406 To estimate TWS changes averaged over the NCP, an averaging kernel based on a calculation
407 that using weighted Gaussian convolution to construct monthly time series from GRACE
408 Stokes coefficients described by equation (5) of Wahr et al. [2014] was used. This method
409 extends the averaging kernel convolution approach [Swenson and Wahr, 2002] by allowing
410 for nonuniform weighting during the convolution. We took the NCP “basin function” from the
411 China provincial boundary grid points and we convolved with a 250 km Gaussian smoothing.
412 We then applied this averaging kernel to GRACE Stokes coefficients to obtain a TWS time
413 series for NCP (Figure 7). The results identified a continuous decrease in TWS from
414 ~~2003~~2004 to 2009; the rate of this decrease slowed towards the end of 2009. The rate of TWS
415 loss obtained by this analysis was 1.62 cm/yr from 2003 to 2009 and 1.23 cm/yr from 2003 to
416 2012 (Table 2).

417

418 The estimated results for the time series analysis also include some contributions outside the
419 NCP due to the finite number of harmonic degrees in the GRACE solution (e.g., $l_{max}=60$ for
420 CSR solutions). The average kernel in our study is also not an exact unity cover for the entire
421 NCP area; these two factors result in under- or overestimation of the true TWS time series
422 signal. To estimate this “leakage in” signal, a scaling factor method was used to restore the
423 amplitude-damped TWS time series. This method, as described by Wahr et al. [2014], requires
424 the construction of a set of simulated Stokes coefficients which represents the signal from a
425 uniformly distributed 1 cm water depth change over the NCP. This estimates a water
426 volume= 3.6626 km^3 based on the overall area of “basin function” (i.e., 366260 km^2). By
427 applying our GRACE analysis procedure to these simulated Stokes coefficients, we can infer
428 an average water thickness change equal to 0.47 cm for the NCP. Each monthly GRACE
429 estimate of NCP water thickness is then multiplied by a scaling factor= $1 \text{ (cm)}/0.47 \text{ (cm)}$ to
430 obtain variations in the total water thickness per area of the NCP. Multiplying the monthly
431 GRACE estimates of NCP water thickness by a scaling factor= $3.6626 \text{ (km}^3\text{)}/0.47 \text{ (cm)}$
432 provides a mass change of the NCP. Table 2 shows the rate of GRACE-derived TWS loss
433 (after multiplying by the scaling factor) in the NCP was 3.39 cm/yr from 2003 to 2009; this is
434 equivalent to a volume of $12.42 \text{ km}^3\text{/yr}$. For a 10-year time span, the rate was 2.57 cm/yr,
435 which is equivalent to a volume of $9.41 \text{ km}^3\text{/yr}$.

436

437 In our study, the GRACE-based TWS time series covers water change~~Loading or unloading~~
438 ~~of the crust from surface mass changes will cause the crust to subside or uplift with different~~
439 ~~amplitudes. These displacements depend on the amplitude of the load and the distance~~

带格式的：字体：11 磅，非加粗

440 ~~between the load and the observation point [Farrell, 1972]. On this basis, we used~~
441 ~~GRACE derived vertical displacements (the method of elastic displacements due to mass~~
442 ~~loads described by Section 2.3) to evaluate TWS loss contributions for the evident crustal~~
443 ~~uplift in the GPS measurements. Time series of monthly predicted vertical surface~~
444 ~~displacements from GRACE for 25 GPS sites in the NCP were plotted (Figure 8a). The fitting~~
445 ~~results (after Least Squares fitting) show the trend rate of GRACE derived vertical~~
446 ~~displacements for the whole region at the 0.37–0.95 mm/yr level from 2004 to 2009, but the~~
447 ~~rate of change direction is inconsistent in different GPS stations at 0.40–0.51 mm/yr level~~
448 ~~from 2010 to 2013 (Table 1). The smoothed results indicate a rising trend from 2004 to 2012~~
449 ~~(Figure 8a) which represented the TWS loss in the observation time span. Figure 8a also~~
450 ~~clearly shows mass anomaly due to TWS changes in the vertical component, e.g., a notable~~
451 ~~negative peak from 2003 to 2005 and subsidence in 2012 (grey background in Figure 8a).~~
452 ~~These GRACE derived long term height fluctuations mainly include variations in the storage~~
453 ~~of natural surface water: high storage in wet years and low storage in dry years [Tang et al.,~~
454 ~~2013], which can be modeled using land surface model output such as those provided by the~~
455 ~~GLDAS [Rodell et al., 2004]. We clearly see that these fluctuations are almost erased by~~
456 ~~removing the modeled soil moisture (SM) of GLDAS/Noah, and the obvious uplift are~~
457 ~~presented in the decomposition of the signal (Figure 8b), which is mainly because the~~
458 ~~contributions from groundwater depletion in the NCP (please see the section 5.1 for discuss in~~
459 ~~details).~~

460

461 ~~5. Discussion~~

5.1 Groundwater Depletion Contributions to Long-Term Uplift

The GRACE derived vertical displacements are also the effect of mass loading sensitive to water at all depths: surface water storage, soil moisture, snow and groundwater, including anthropogenic effects (i.e., groundwater withdrawal, inter-basin diversion, reservoir and coal transport). To isolate the groundwater contributions, the Noah version of GLDAS which possesses monthly intervals and spatial resolution of 1.0 degrees [Rodell et al., 2004] was used to subtract monthly water storage estimates predicted by land surface models. GLDAS generates a series of land surface forcing (e.g., precipitation, surface meteorology and radiation), state (e.g., soil moisture and temperature, and snow), and flux (e.g., evaporation and sensible heat flux) data simulated by land surface models. The GLDAS/Noah model can provide values of snow, vegetation and all soil moisture layers, but it does not include anthropogenic and climate-driven groundwater depletion. So we isolated GWS variations by groundwater contributions retained in heights time series when GRACE derived vertical displacements subtracting simulated SM data from GLDAS/Noah model from GRACE-derived total TWS effects.

In order to confirm validation of the results in this study, our GRACE-based estimate was compared with field measurement data of groundwater level (e.g., in situ water table observations) and the results from previous studied (e.g., the reported TWS loss from Zhong et al. [2009], Su et al. [2011], Moiwo et al. [2009], and the reported GWS loss from Huang et al. [2015], Feng et al. [2013], Tang et al. [2013]). We have acquired in situ groundwater level measurements (most of groundwater table depth in the shallow unconfined aquifers, available

带格式的: 字体: 12 磅, 加粗

484 from 2002 to 2013), which are mainly located in the central and eastern plain of the NCP
485 (including the Beijing, Tianjin and some cities of Hebei, Henan and Shandong province). The
486 data series are obtained from Ministry of Water Resources of China (MWR) (available at:
487 <http://sqqx.hydroinfo.gov.cn/shuiziyuan/>). We get the area-weighted mean groundwater level
488 change series in the NCP from time series of monthly groundwater table depth changes of 20
489 cities in our study region. We also collected the daily precipitation data (rainfall amount) for
490 weather stations during the period of 2003~2012 from China Meteorological Data Sharing
491 Service System (CMDSSS) (available at: <http://cdc.cma.gov.cn/index.jsp>). Figure 7 shows our
492 GRACE-based estimate is generally consistent with that monthly groundwater level changes
493 observed by monitoring wells after multiplying by mean value of specific yields in the NCP
494 during 2002~2012.

495
496 Note that our GRACE-based TWS time series covers all depth of water mass changes and
497 most of the groundwater level changes from observations of shallow aquifers, which showed
498 the long-term mass loss in the NCP from 2003 to 2009, but the rate of this decrease slowed
499 towards the end of 2009 and then increases again after 2010. This difference in two
500 sub-periods (2004~2009 and 2010~2012) is mainly induced by climate-driven precipitation
501 recharge in NCP (Figure 7). In addition, comparison between monthly GWS variations
502 estimated from GRACE minus GLDAS/Noah model and in situ groundwater level
503 measurements also confirmed the difference of trend changes of GWS in these two
504 sub-periods (Table 2). The rate of GRACE-derived GWS loss (after multiplying by the
505 scaling factor) in the NCP was 2.49 cm/yr from 2003 to 2009 and 2.72 cm/yr from 2003 to

506 2009; this is equivalent to a volume of 9.12 km³/yr and 9.96 km³/yr, respectively. Our
507 GRACE-based depletion of groundwater was significantly higher than ground-based
508 measurements. Although the shallow GWS increase from 2010 to 2012 due to precipitation
509 recharge in NCP, but the increase of rainfall is difficult to recharge the current more serious
510 depletion of groundwater in the deep aquifers.

511
512 In addition, we compare the depletion in TWS or GWS between our results and previous
513 studied results. Table 2 shows our results and compare them with the earlier analysis in
514 different zones where TWS or GWS loss surveys have been published. We found that the
515 trend rate of our GRACE-based GWS in the whole NCP region is in good agreement with that
516 reported by Huang et al. [2015] during 2003~2012 and Feng et al. [2013] during 2003~2010,
517 which are estimated from the level 2 Release-05 GRACE data and multiplied by the scaling
518 factor. However, other previous results showed obvious difference between the loss rate of
519 TWS and GWS because these studies used the early versions of the GRACE data, different
520 defined area of NCP or do not use scaling factor compared with Huang's, Feng's and our
521 study. For instance, Zhong et al. [2009] found a rate of 2.4 cm/yr from 2003 to 2007 based on
522 level 2 Release-04 GRACE data in Beijing, Hebei and Tianjin; Su et al. [2009] calculated
523 TWS and GWS declining at a rate of 1.1 cm/yr and 0.5 cm/yr from 2002 to 2010, respectively,
524 based on level 2 Release-04 GRACE data in Beijing, Tianjin, Hebei, Shandong, and Henan;
525 and Moiwo et al. [2013] estimated a TWS loss rate of 1.68 cm/yr from 2002 to 2009 in the
526 vast north China (i.e., in addition to Beijing and Tianjin, the study area is comprised of 12
527 other provinces). Although Tang et al. [2013] did not applied scaling factor to restore the

528 amplitude-damped GRACE signal, but they used the latest GRACE products (RL05) and
529 same region of NCP with our study. Thus, Tang et al. [2013] estimated a GWS depletion rate
530 of 0.84 to 1.4 cm/yr (2003~2011) is also in good agreement with our estimated result before
531 being multiplied by scaling factor (i.e., the rate of TWS loss was 1.23 cm/yr from 2003 to
532 2012).

533

534 **4.2 Groundwater Depletion Contributions to Long-Term Uplift**

535 Loading or unloading of the crust from surface mass changes will cause the crust to subside or
536 uplift with different amplitudes. These displacements depend on the amplitude of the load and
537 the distance between the load and the observation point [Farrell, 1972]. On this basis, we used
538 GRACE-derived vertical displacements (the method of elastic displacements due to mass
539 loads described by Section 2.3) to evaluate TWS loss contributions for the evident crustal
540 uplift in the GPS measurements. Time series of monthly predicted vertical surface
541 displacements from GRACE for 25 GPS sites in the NCP were plotted (Figure 8a). The fitting
542 results (after Least-Squares fitting) show the trend rate of GRACE-derived vertical
543 displacements for the whole region at the 0.37~0.95 mm/yr level from 2004 to 2009, but the
544 rate of change direction is inconsistent in different GPS stations at -0.40~0.51 mm/yr level
545 from 2010 to 2013 (Table 1). The smoothed results indicate a rising trend from 2004 to 2012
546 (Figure 8a) which represented the TWS loss in the observation time span. Figure 8a also
547 clearly shows mass anomaly due to TWS changes in the vertical component, e.g., a notable
548 negative peak from 2003 to 2005 and subsidence in 2012 (grey background in Figure 8a).
549 These GRACE-derived long-term height fluctuations mainly include variations in the storage

550 of natural surface water: high storage in wet years and low storage in dry years [Tang et al.,
551 2013], which can be modeled using land surface model output such as those provided by the
552 GLDAS [Rodell et al., 2004].

553

554 Figure 8b shows the GRACE-derived height amplitudes after removing the continental water
555 storage signal which uses the using output from the GLDAS/Noah hydrology model, ~~to~~
556 ~~remove the continental water storage signal.~~ The calculated results show that the contributions
557 of other types of TWS effects (except groundwater) on the surface are small relative to
558 groundwater depletion, and those main loading loads mainly effects on the amplitudes of
559 seasonal displacement with no obvious long-term trend. Meanwhile, we clearly see that these
560 fluctuations (grey background in Figure 8a) are almost erased from the GRACE-derived
561 minus GLDAS/Noah vertical displacements, and the obvious continuous uplift are presented
562 in grey background of Figure 8b, which is mainly because the contributions from groundwater
563 depletion in the NCP. Contrasts between Compare the seasonal amplitudes, phases and
564 trend trend fit of vertical displacement derived by GRACE displacements between before and
565 after removing remove GLDAS/Noah effects and the original ones. Please from
566 ~~GRACE derived displacement, please~~ see the Table S4 in the supporting information.

带格式的: 字体颜色: 红色

带格式的: 字体颜色: 红色

带格式的: 字体颜色: 红色

带格式的: 字体颜色: 红色

567

568 For the results described above, after the subtraction of the GLDAS/Noah contributions,
569 GRACE-derived heights largely reflect loading effects from the groundwater (natural and
570 anthropogenic factors) and anthropogenic contributions. The anthropogenic impact on mass
571 change was investigated by Tang et al. [2013] for the effect of inter-basin diversion, reservoir

572 and coal transport distribution on the GRACE-derived estimates of groundwater depletion in
573 the NCP. Results from their investigation showed that the trend of anthropogenic
574 contributions was equivalent to 4.83 mm/yr water thickness (described by equations in Table
575 2 of Tang et al. [2013]) during 2003–2011 for the whole NCP. This means that there was a
576 large groundwater depletion contribution for the GRACE-derived vertical displacements in
577 long-term uplift. Investigating groundwater withdrawal due to anthropogenic activities
578 (drinking water extraction, agricultural irrigation and industrial manufacturing) should be of
579 high importance because precipitation data for this area (~~shown in Figure 7~~~~(provided by the~~
580 ~~China Meteorological Data Sharing Service System, available at <http://cdc.nmic.cn/home.do>)~~)
581 indicated no long-term droughts during the GRACE observation period of 2003–2011.

582

583 5. Discussion

584 5.1 The Loading Effects of Non-tidal Ocean and Atmospheric Variations

585 As part of the processing performed by the GRACE Project, the GRACE Stokes coefficients
586 (denoted by the GRACE Project as “GSM” coefficients) have had modeled estimates of the
587 atmospheric and oceanic mass signals removed. Thus the GRACE coefficients include the full
588 effects of terrestrial water storage. The GRACE Project provides the modeled atmospheric
589 and oceanic contributions to the Stokes coefficients in two forms: “GAC” files which include
590 the global atmospheric and oceanic effects, and “GAD” files which have had the atmospheric
591 signals over land set to zero. The coefficients in the GAD file therefore represent ocean
592 bottom pressure variations. “GAA” files are those add CSR's GAC files to the GSM files, and
593 subtract the GAD files. The coefficients in the GAA file represent atmospheric pressure

594 variations.

595

596 As is mentioned in Section 1, the cause of the difference between our results and Liu's work

597 [Liu et al., 2014] is we removed atmospheric and non-tidal ocean loading effects while they

598 did not. However, we found that the amplitude of GPS after removing atmospheric and

599 non-tidal ocean loading effects, is still greater than the GRACE while we added the AOD1B

600 (GAC solution) de-aliasing model to the GRACE solutions (i.e., no atmospheric and non-tidal

601 ocean corrected, please see the Table S1 in the supporting information). The most obvious

602 difference between our results and Liu's work [Liu et al., 2014] is that they adopt the load

603 Love numbers from Guo et al. [2004] to transform these coefficients into vertical surface

604 displacement estimates. We check the two results of Love numbers (ocean-load and

605 atmospheric pressure-load) from Guo et al. [2004], there are significant differences between

606 ocean-load and atmospheric pressure-load Love numbers. Meanwhile, we compared k_2 Love

607 numbers from Guo et al. [2004] (Liu et al.'s work) and k_2 Love numbers from Han and Wahr

608 [1995] (our work) with the k_2 Love numbers used in AOD1B products [Farrell, 1972],

609 respectively. The different Love numbers have caused the amplitude of the same station from

610 Liu's GRACE-derived vertical displacements much more than GPS and our GRACE results,

611 due to k_2 from atmospheric pressure-load Love numbers [Guo et al., 2004] significantly larger

612 than Love numbers from Han and Wahr [1995] and Farrell [1972]. The detailed analysis of

613 the different Love numbers from Guo et al. [2004], Han and Wahr [1995] and Farrell [1972],

614 please see the Section S1 in the supporting information. Moreover, Table S3 in the supporting

615 information indicate that our correlation results of IGS stations (BJFS, BJSH, JIXN, TAIN

616 and ZHNZ) are consistent with Liu's work [Liu et al., 2014], indicating that the seasonal
617 variations might come from the same geophysical process. The WRMS residual reduction
618 ratio for all the stations ranged from 19% to 85%, which is better than Liu's work [Liu et al.,
619 2014]. However, the correlation and WRMS reduction between GPS and GRACE are weak
620 when atmospheric and non-tidal ocean effects was removed, with the average correlation and
621 WRMS reduction reduce to 75.6% and 28.9%, respectively. This is mainly because the
622 seasonal hydrologic process is major contributors to seasonal changes, and different stations
623 are greatly influenced by the surrounding hydrological process.

624

625 **5.2 Removing Hydrological Loading Displacement from GPS Using GRACE Data**

626 Coordinate variations measured by GPS stations, principally for the vertical component, have
627 been used to investigate global [Dong et al., 2002] and local [Grapenthin et al., 2006] tectonic
628 activity, as well as seasonal displacement modes for constraining estimates of continental,
629 atmospheric and ocean water storage. Some previous studies [e.g., Fu et al., 2012] have
630 focused on the vertical component of crustal motion with relying on the accurate
631 interpretation of GPS motion in terms of surface stress or tectonic movement. Thus, the
632 displacement signal from surface mass loading is a source of noise [van Dam et al., 2007].
633 For these applications, they would like to obtain reliable loading models or even surface mass
634 observations, which can be used to reduce the environmental loading contributions to the GPS
635 observations. In this study, we also attempt to separate tectonic and hydrological effect using
636 GRACE-derived hydrological vertical rates. As mentioned in the Section 3, the good seasonal
637 correlation between GRACE and GPS signals indicates that the long-term uplifts revealed by

638 GRACE detections are probably true and mixed in the GPS measurements.

639

640 Figure 9 shows results for individual GPS time series. Crustal subsidence or uplift due to
641 vertical tectonic motion and TWS changes in the studied period are clearly evident in the
642 vertical component shown in most of the GPS stations; In fact, the analysis in the five IGS
643 GPS stations (BJFS, BJSH, JIXN, TAIN and ZHNZ) suggests that the GPS vertical time
644 series can be described by two different rates around 2010, due to a continuous decrease in
645 TWS from 2004 until 2009; towards the end of 2009 the rate of this decrease slowed and rate
646 started to rise since 2010 (please see Figure 6). Thus, we divided it into two sub-periods when
647 fitting GPS and GRACE trend for these five stations (Figure 9a). GPS trend changes indicate
648 an overall uplift for the whole region at the $0.04 \sim 1.47$ mm/yr level from 2004 to 2009, but
649 the rate of change direction is inconsistent in different GPS stations at $-0.94 \sim -2.55$ mm/yr
650 level from 2010 to 2013 (Table 1).

651

652 In addition, the long-term trend rate is different in different areas from 2010 to 2013 (Figure
653 9b). For example, the trend rate from GPS measurements shows the uplift in western NCP
654 (Shanxi-SX, and some of Hebei-HE stations), but opposite trends in the central and eastern
655 plain of NCP (Beijing-BJ, Tianjin-TJ and some of Hebei-HE stations). The groundwater
656 depletion which occurs in the shallow unconfined aquifers in Piedmont Plain leads to the
657 loading uplift effect from mass loss. But groundwater depletion occurs in the deep confined
658 aquifers in the central and eastern plain of NCP, which causes serious ground subsidence,
659 rather than ground uplift caused by groundwater loss.

660

661 It is also possible that some GPS signals could be a result of loading from changes in the
662 distribution of water stored in the surface and ground around the GPS surrounding region. To
663 remove those contributions, Stokes coefficients output from the GRACE model were used to
664 compute crustal motion at the NCP (Figure 8a), and then transform the monthly results into
665 daily resolution data using a spline interpolation. In addition, GRACE solutions are corrected
666 for GIA while GPS ones are not. Here Stokes coefficients results from A et al. [2013] were
667 used to remove GIA effects from GPS measurements, which is about 0.2--0.4 mm/year in the
668 land areas of China and 0.28--0.33 mm/year in the NCP (Please see the Figure S5 and Table
669 S4 in the supporting information).

670

671 We compute the GRACE-derived long-term uplift for all continuous GPS sites used in this
672 paper. The results indicate an overall uplift for the NCP region. Then we remove this TWS
673 induced uplift from GPS actual observed vertical rates to derive the corrected vertical
674 velocities. Figure 10 divided the time into two sub-periods (2004--2009 and 2010--2013) to
675 indicate an overall long-term trend before (gray arrow) and after (red arrow) removing
676 hydrological loading displacement for the whole region. Secular displacement results between
677 2004 and 2009 show that loading displacement due to the TWS loss reduce the uplift rate of
678 GPS to some extent, and groundwater exploitation was the main contributor to crustal uplift
679 caused by TWS loss in the NCP (BJFS, BJSH and JIXN in the Figure 10a). However, studies
680 indicate that groundwater withdrawal produces localized subsidence which can be largely
681 relative to tectonic displacement [Bawden et al., 2001]. Therefore, in this study, more

682 attention was paid to land subsidence due to groundwater loss.

683

684 **5.3 Land subsidence in the central and eastern of NCP**

685 Land subsidence has been commonly observed in the NCP, and has become the main factor
686 that impacts regional sustainable economic and social development [Guo et al., 2015]. Over
687 the past years, the scope and magnitude of land subsidence has expanded. In this study, we
688 used GPS sites to obtain time series of land subsidence evolution characteristics. The trend
689 rates from GPS sites, after removing the rates from GRACE-derived long-term uplift and GIA
690 effects can be seen in Figure 10b (the gray background areas in the dashed white box) to
691 reflect the rate of land subsidence from 2010 to 2013, which is because the groundwater
692 exploitation in the deep confined aquifers has a more serious impact on land subsidence [Guo
693 et al., 2015]. The results show that Tianjin becomes the most serious subsidence area, e.g., in
694 the Tanggu and Hangu district (TJBH), with an average subsidence of ~14 mm/yr after 2010;
695 In Wuqing district (TJWQ), recent subsidence averaged ~43 mm/yr. Because the Cangxian
696 district (HECX) is close in proximity to the Jinghai region of Tjian, the sedimentation rate of
697 ~20 mm/yr can represent the subsidence trend of southwest Tianjin. However, the difference
698 of spatial distribution of land subsidence is large in Tianjin, and uneven settlement
699 characteristics are obvious. For example, the southwest and western areas of Tianjin are the
700 most serious areas, and the trend of land subsidence exists in the northward but the amplitude
701 is small relative to the southwest and western areas, i.e., (JIXN site shows a small negative
702 trend ~~~~~ -0.6 mm/yr). The cause for subsidence in the Tianjin area is linked to over
703 exploitation of groundwater, an issue that has not been effectively controlled resulting in

704 rapidly developing land subsidence in the suburbs in recent years [Yi et al., 2011].

705

706 In the central and eastern region of NCP, where disastrous land subsidence has also occurred
707 in Beijing and cities in central of Hebei province and the northeast of Shandong province, for
708 instance, large subsidence zone in Hebei province has formed from north to south, where start
709 from the western region of Beijing (BJFS, BJSH and BJYQ station), via the eastern region of
710 Xingtai and Handan (HELY station), extend to the northern of Hebi (HAHB station belong to
711 Henan province).

712

713 However, results from our investigation show that the center of land subsidence does not
714 completely overlap the TWS loss contributions (see the secular trend maps of the TWS
715 changes of NCP in Figure 2). The uplift still exists even when we removed the rates from
716 GRACE-derived and GIA effects in the piedmont of Taihang Mountains and the western part
717 of NCP (Shanxi province), where the groundwater depletion occurs in the shallow unconfined
718 aquifers have not led to a large area of subsidence. The reason for this difference with the
719 western region of NCP is that crustal uplift is mainly controlled by tectonic movement, which
720 is the orogenic belt and plateau area in western of the Taihang Mountains basic in the uplift.
721 In our results, most of the corrected vertical velocities at GPS stations, especially in the
722 central and eastern region of NCP, agree with the previous study results, i.e., combining with
723 mobile and continuous GPS observation [Zhao et al., 2014] and using GPS stations from
724 GNSS and leveling data [MLR, 2015], The results of vertical crust movement in the NCP
725 from the previous study, please see the Figure S6 in the supporting information.

726

727 **6. Conclusions**

728 Temporal variations in the geographic distribution of surface mass (continental water, ocean
729 mass and atmospheric mass) can lead to displacement of the Earth's surface. Due to excessive
730 exploitation of groundwater resources the NCP area has become susceptible to land
731 subsidence, and it has become one of the most affected areas in the world. Calculating the
732 loading displacement can explain the natural displacement phenomenon, and it presents new
733 insight into the dynamics of land subsidence.

734

735 Traditional displacement observation has space limitations. Based on the elastic displacement
736 of the Earth's crust by surface loadings, this study combined GRACE and GPS data to
737 investigate vertical displacements in the NCP area. GRACE data was used to model vertical
738 displacements due to changes in hydrological loads. The results showed both GPS and
739 GRACE data to observe strong seasonal variations. Comparisons between the observed GPS
740 seasonal vertical displacement and GRACE-derived seasonal displacement demonstrated that
741 a consistent physical mechanism is responsible for TWS changes, i.e., the seasonal
742 hydrospheric mass movements due to climate variability cause periodic displacements of the
743 lithosphere.

744

745 As well as the significant seasonal characteristics, GRACE also exhibited a long-term mass
746 loss in this region; the rate of GRACE-derived TWS loss (after multiplying by the scaling
747 factor) in the NCP was 3.39 cm/yr from 2003 to 2009, which is equivalent to a volume of

748 12.42 km³/yr. The rate was 2.57 cm/yr from 2003 to 2012, equivalent to a volume of 9.41
749 km³/yr. The TWS loss was principally due to groundwater depletion in the NCP. We
750 calculated that the consequent trend rate caused by the load mass change using GRACE data
751 and removed this hydrological effect from observed GPS vertical rates. Secular displacement
752 results showed that TWS losses reduced loading displacement to some extent, but the trend
753 rates disagree due to the difference of spatial distribution with anthropogenic depletion of
754 TWS in the NCP.

755

756 Particularly, land subsidence has been affecting the central and eastern region of NCP,
757 especially in Tianjin for the past years. Over-pumping of groundwater is the main cause of
758 land subsidence which has led to comprehensive detrimental effects on the society, the
759 economy and the natural environment. The impact of groundwater exploitation in different
760 aquifer systems and active faults in the different regions on land subsidence needs to be
761 analyzed in future investigations. For example, using GRACE to remove mass loading signals
762 from a GPS record requires either confidence that there is no concentrated load signal very
763 near the site, or a scaling factor based on a reliable model of the mass change (the
764 groundwater depletion rate estimated from monitoring well stations) pattern around the site.

765

766 **Acknowledgments.** The GPS data of CMONOC and IGS were made by First Crust
767 Monitoring and Application Center, China Earthquake Administration
768 (<http://www.eqdsc.com/data/pgv-sjxl.htm>). [The groundwater level data series were obtained](#)
769 [from MWR \(<http://sqqx.hydroinfo.gov.cn/shuiziyuan/>\), and the daily precipitation data for](#)

770 ~~weather stations were collected from CMDSSS (<http://cdc.cma.gov.cn/index.jsp>). We also~~
771 ~~thank NASA~~~~We also thank the Center of Space Research (CSR) teams~~ for their online
772 accessible GRACE solutions (<ftp://podaac.jpl.nasa.gov/allData/grace/L2/CSR/RL05/>) and the
773 GLDAS/Noah model data provided by the NASA Goddard Earth Sciences Data and
774 Information Services Center (<http://disc.sci.gsfc.nasa.gov/>). This work was initiated while L.
775 Wang was visiting Prof. John Wahr at the Department of Physics, University of Colorado at
776 Boulder. We are grateful to Prof. John Wahr for his helpful suggestions, including estimating
777 the TWS changes averaged over the NCP using averaging kernel method and loading
778 responses due to water change using GRACE Stokes coefficients to calculate the elastic
779 displacement. This work is supported by the National Natural Science Foundation of China
780 (NSFC) (Grant No. 41504065, ~~41574070, 41604060~~), China Postdoctoral Science Foundation
781 funded project (Grant No. 2014T70753), ~~and~~ the [Fundamental Research Funds for the Central](#)
782 [Universities](#), China University of Geosciences (~~WuhanCUG~~) ~~Hubei Subsurface Multi-scale~~
783 ~~Imaging Lab (Grant No. SMIL-2014-09)~~ and Hubei province natural science foundation of
784 ~~China (Grant No. 2014CFB170)~~.

785

786 **References**

787 A, G., Wahr, J., Zhong, S., 2013. Computations of the viscoelastic response of a 3-D
788 compressible earth to surface loading: An application to glacial isostatic adjustment in
789 Antarctica and Canada. *Geophys. J. Int.* 192, 557–572. doi: 10.1093/gji/ggs030.

790 Altamimi, X., Collilieux, X., Metivier, L., 2011. ITRF2008: An improved solution of the
791 International Terrestrial Reference Frame. *J. Geod.* 85(8), 457–473. doi:

792 10.1007/s00190-011-0444-4.

793 Bawden, G.W., Thatcher, W., Stein, R.S., Wicks, C., Hudnut, K., Peltzer, G., 2001. Tectonic
794 contraction across Los Angeles after removal of groundwater pumping effects. *Nature* 412,
795 812–815. doi: 10.1038/35090558.

796 Bevis, M., Alsdorf, D., Kendrick, E., Fortes, L.P., Forsberg, B., Smalley Jr., R., Becker, J.,
797 2005. Seasonal fluctuations in the mass of the Amazon River system and Earth's elastic
798 response. *Geophys. Res. Lett.* 32, L16308. doi: 10.1029/2005GL023491.

799 Blewitt, G., 2003. Self-consistency in reference frames, geocenter definition, and surface
800 loading of the solid Earth. *J. Geophys. Res.*, 108(B2). doi: 10.1029/2002JB002082.

801 Boehm, J., Heinkelmann, R., Schuh, H., 2007. Short note: A global model of pressure and
802 temperature for geodetic applications. *J. Geod.* 81, 679–683. doi:
803 10.1007/s00190-007-0135-3.

804 Chao, B.F., Wu, Y., Li, Y., 2008. Impact of artificial reservoir water impoundment on global
805 sea level. *Science* 320, 212–214. doi: 10.1126/science.1154580.

806 Cheng, M.K., Tapley, B.D., Ries, J.C., 2013. Deceleration in the earth's oblateness. *J.*
807 *Geophys. Res.* 118, 1–8. doi: 10.1002/jgrb.50058.

808 Döll, P., 2009. Vulnerability to the impact of climate change on renewable groundwater
809 resources: a global-scale assessment. *Environ. Res. Lett.* 4, 036006. doi:
810 10.1088/1748-9326/4/3/035006.

811 Döll, P., Kaspar, F., Lehner, B., 2003. A global hydrological model for deriving water
812 availability indicators: Model tuning and validation. *J. Hydrol.* 270, 105–134.

813 Dong, D., Fang, P., Bock, Y., Cheng, M.K., Miyazaki, S., 2002. Anatomy of apparent seasonal

814 variations from GPS-derived site position time series. *J. Geophys. Res.* 107(B4), 2075. doi:
815 10.1029/2001JB000573.

816 Farrell, W.E., 1972. Deformation of the Earth by surface loadings. *Rev. Geophys. Space Phys.*
817 10, 761–797. doi: 10.1029/RG010i003p00761.

818 Feng, W., Zhong, M., Lemoine, J.M., Biancale, R., Hsu, H.T., Xia, J., 2013. Evaluation of
819 groundwater depletion in North China using the Gravity Recovery and Climate Experiment
820 (GRACE) data and ground-based measurements. *Water Resour. Res.* 49, 2110–2118. doi:
821 10.1002/wrcr.20192.

822 Fu, Y., Argus, D.F., Freymueller, J.T., Heflin, M.B., 2013. Horizontal motion in elastic
823 response to seasonal loading of rain water in the Amazon Basin and monsoon water in
824 Southeast Asia observed by GPS and inferred from GRACE. *Geophys. Res. Lett.* 40. doi:
825 10.1002/2013GL058093.

826 Fu, Y., Freymueller, J.T., 2012. Seasonal and long-term vertical deformation in the Nepal
827 Himalaya constrained by GPS and GRACE measurements. *J. Geophys. Res.* 117, B03407. doi:
828 10.1029/2011JB008925.

829 Fu, Y., Freymueller, J.T., and van Dam, T., 2012. The effect of using inconsistent ocean tidal
830 loading models on GPS coordinate solutions. *J. Geod.*, 86(6), 409–421. doi:
831 10.1007/s00190-011-0528-1.

832 Grapenthin, R., Sigmundsson, F., Geirsson, H., Árnadóttir, T., Pinel, V., 2006. Icelandic
833 rhythmic: Annual modulation of land elevation and plate spreading by snow load. *Geophys.*
834 *Res. Lett.* 33, L24305. doi: 10.1029/2006GL028081.

835 Guo, H., Zhang, Z., Cheng, G., Li, W., Li, T., Jiao, J. J., 2015. Groundwater-derived land

836 subsidence in the north china plain. *Environ. Earth Sci.* 74, 1415–1427. doi:
837 10.1007/s12665-015-4131-2.

838 Guo, J.Y., Li, Y.B., Huang, Y., Deng, H.T., Xu, S.Q., Ning, J.S., 2004. Green's Function of
839 Earth's Deformation as a Result of Atmospheric Loading. *Geophys. J. Int.*, 159, 53–68. doi:
840 10.1111/j.1365-246X.2004.02410.x.

841 Han, D., and Wahr, J., 1995. The viscoelastic relaxation of a realistically stratified Earth, and
842 a further analysis of post-glacial rebound. *Geophys. J. Int.*, 120, 287–311.

843 Hao, M., Freymueller, J.T., Wang, Q.L., Cui, D.X., Qin, S.L., 2016. Vertical crustal movement
844 around the southeastern Tibetan Plateau constrained by GPS and GRACE data. *Earth Planet.*
845 *Sci. Lett.*, 437(5107), 1–8. doi: 10.1016/j.epsl.2015.12.038.

846 Heki, K., 2001. Seasonal modulation of interseismic strain buildup in north-eastern Japan
847 driven by snow loads. *Science* 293, 89–92. doi: 10.1126/science.1061056.

848 Huang, Z., Pan, Y., Gong, H., Yeh, P.J.F., Li, X., Zhou, D., Zhao, W., 2015. Subregional-scale
849 groundwater depletion detected by GRACE for both shallow and deep aquifers in North
850 China Plain. *Geophys. Res. Lett.* 42, 1791–1799. doi: 10.1002/2014GL062498.

851 Joodaki, G., Wahr, J., Swenson, S., 2014. Estimating the human contribution to groundwater
852 depletion in the Middle East, from GRACE data, land surface models, and well observations.
853 *Water Resour. Res.* 50, 2679–2692. doi: 10.1002/2013WR014633.

854 Khan, S.A., Wahr, J., Bevis, M., Velicogna, I., Kendrick, E., 2010. Spread of ice mass loss
855 into northwest Greenland observed by GRACE and GPS. *Geophys. Res. Lett.* 37, L06501. doi:
856 10.1029/2010GL042460.

857 Kusche, J., Schrama, E.J.O., 2005. Surface mass redistribution inversion from global GPS

858 deformation and Gravity Recovery and Climate Experiment (GRACE) gravity data. *J.*
859 *Geophys. Res.* 110, B09409. doi: 10.1029/2004JB003556.

860 Liu, R.L., Li, J.C., Fok, H.S., Shum, C.K., Li, Z., 2014. Earth surface deformation in the
861 North China Plain detected by joint analysis of GRACE and GPS data. *Sensors* 14,
862 19861-19876. doi: 10.3390/s141019861.

863 Ministry of Land and Resources of China (MLR), 2015. Monitoring results of important
864 geographical conditions in the Beijing-Tianjin-Hebei region, Ministry of Land and Res. of
865 China, Beijing. [Available at <http://www.mlr.gov.cn/>].

866 Moiwo, J.P., Tao, F., Lu, W., 2013. Analysis of satellite-based and in situ hydro-climatic data
867 depicts water storage depletion in North China Region. *Hydrol. Process.* 27, 1011–1020. doi:
868 10.1002/hyp.9276.

869 Nielsen, K., Khan, S.A., Spada, G., Wahr, J., Bevis, M., Liu, L., van Dam, T., 2013. Vertical
870 and horizontal surface displacements near Jakobshavn Isbræ driven by melt-induced and
871 dynamic ice loss. *J. Geophys. Res. Solid Earth* 118, 1837–1844. doi: 10.1002/jgrb.50145.

872 Oleson, K. W., et al., 2013. Technical description of version 4.5 of the Community Land
873 Model (CLM), NCAR Tech. Note NCAR/TN-5031STR, 434 pp, National Center for
874 Atmospheric Research, Boulder, Colorado.

875 Peltier, W.R., 2004. Global glacial isostasy and the surface of the ice-age earth: The ice-5G
876 (VM2) model and GRACE. *Annu. Rev. Earth Planet. Sci.* 32, 111-149.

877 Rodell, M., et al., 2004. The global land data assimilation system. *Bull. Am. Meteorol. Soc.*
878 85, 381–394. doi: 10.1175/BAMS-85-3-381.

879 Rodell, M., Velicogna, I., Famiglietti, J.S., 2009. Satellite-based estimates of groundwater

880 depletion in India. *Nature* 460, 999–1002. doi: 10.1038/460789a.

881 Sauber, J., Plafker, G., Molnia, B.F., Bryant, M.A., 2000. Crustal deformation associated with
882 glacial fluctuations in the eastern Chugach Mountains, Alaska. *J. Geophys. Res. Solid Earth*
883 105(B4), 8055–8077. doi: 10.1029/1999JB900433.

884 [Su, X.L., Ping, J.S., Ye, Q.X., 2011. Terrestrial water variations in the North China Plain](#)
885 [revealed by the GRACE mission, *Sci. China Earth Sci.*, 54 \(12\), 1965–1970.](#)
886 [doi:10.1007/s11430-011-4280-4.](#)

887 Swenson, S., Chambers, D., Wahr, J., 2008. Estimating geocenter variations from a
888 combination of GRACE and ocean model output. *J. Geophys. Res.* 113, B08410. doi:
889 10.1029/2007JB005338.

890 Swenson, S., Wahr, J., 2002. Methods for inferring regional surface-mass anomalies from
891 Gravity Recovery and Climate Experiment (GRACE) measurements of time-variable gravity,
892 *J. Geophys. Res.*, 107(B9), 2193. doi: 10.1029/2001JB000576.

893 Swenson, S., Wahr, J., 2006. Post-processing removal of correlated errors in GRACE data.
894 *Geophys. Res. Lett.*, 31: L23402. doi: 10.1029/2005GL025285.

895 Syed, T.H., Famiglietti, J.S., Rodell, M., Chen, J., Wilson, C.R., 2008. Analysis of terrestrial
896 water storage changes from GRACE and GLDAS. *Water Resour. Res.* 44, W02433. doi:
897 10.1029/2006WR005779.

898 Tang, Q., Zhang, X., Tang, Y., 2013. Anthropogenic impacts on mass change in North China.
899 *Geophys. Res. Lett.* 40, 3924–3928. doi: 10.1002/grl.50790.

900 Tapley, B.D., Bettadpur, S., Watkins, M., Reigber, C., 2004a. The gravity recovery and
901 climate experiment: Mission overview and early results. *Geophys. Res. Lett.* 31, L09607. doi:

902 10.1029/2004GL019920.

903 van Dam, T., 2010. NCEP Derived 6 hourly, global surface displacements at 2.5×2.5 degree
904 spacing. <http://geophy.uni.lu/ncep-loading.html>.

905 van Dam, T., Blewitt, G., Heflin, M., 1994. Detection of atmospheric pressure loading using
906 the Global Positioning System. *J. Geophys. Res.* 99(B12): 23939–23950.

907 van Dam, T., Collilieux, X., Wuite, J., Altamimi, Z., Ray, J., 2012. Nontidal ocean loading:
908 Amplitudes and potential effects in GPS height time series. *J. Geod.* 86, 1043–1057. doi:
909 10.1007/s00190-012-0564-5.

910 van Dam, T., Wahr, J., Lavallée, D., 2007. A comparison of annual vertical crustal
911 displacements from GPS and Gravity Recovery and Climate Experiment (GRACE) over
912 Europe. *J. Geophys. Res.* 112, B03404. doi: 10.1029/2006JB004335.

913 Wahr, J., Khan, S.A., van Dam, T., Liu, L., van Angelen, J.H., van den Broeke, M.R.,
914 Meertens, C.M., 2013. The use of GPS horizontals for loading studies, with applications to
915 northern California and southeast Greenland. *J. Geophys. Res. Solid Earth* 118, 1795–1806.
916 doi: 10.1002/jgrb.50104.

917 Wahr, J., Molenaar, M., Bryan, F., 1998. Time-variability of the earth's gravity field:
918 Hydrological and oceanic effects and their possible detection using GRACE. *J. Geophys. Res.*
919 103, 30205–30230.

920 Wahr, J., Smeed, D.A., Leuliette, E., Swenson, S., 2014. Seasonal variability of the Red Sea,
921 from satellite gravity, radar altimetry, and in situ observations. *J. Geophys. Res. Oceans* 119,
922 5091–5104. doi: 10.1002/2014JC010161.

923 Wang, L.S., Chen, C., Du, J.S., Wang, Q.G., Sun, S.D., 2014. Impact of China large reservoir

924 water impoundment on spatial variability of coastal relative sea level. *Earth Sci.* (in Chinese
925 with an English abstract) 39(11), 1607–1616. doi: 10.3799/dqkx.2014.154.

926 Wang, L.S., Chen, C., Zou, R., Du, J.S., 2014. Surface gravity and deformation effects of
927 water storage changes in China's Three Gorges Reservoir constrained by modeled results and
928 in situ measurements. *J. Appl. Geophys.* 108, 25–34. doi: 10.1016/j.jappgeo.2014.06.007.

929 Wang, L.S., Chen, C., Zou, R., Du, J.S., Chen, X.D., 2014. Using GPS and GRACE to detect
930 seasonal horizontal deformation caused by loading of terrestrial water: A case study in the
931 Himalayas. *Chinese J. Geophys.* (in Chinese with an English abstract) 57(6), 1792–1804. doi:
932 10.6038/cjg20140611.

933 Wang, M., Li Q., Wang, F., Zhang, R., Wang, Y.Z., Shi, H.B., Zhang, P.Z., Shen, Z.K., 2011.
934 Far-field coseismic displacements associated with the 2011 Tohoku-oki earthquake in Japan
935 observed by Global Positioning System. *Chinese Sci. Bull.*, 56, 2419–2424. doi:
936 10.1007/s11434-011-4588-7.

937 Wang, X., de Linage, C., Famiglietti, J., Zender, C.S., 2011. Gravity Recovery and Climate
938 Experiment (GRACE) detection of water storage changes in the Three Gorges Reservoir of
939 China and comparison with in situ measurements. *Water Resour. Res.* 47, W12502. doi:
940 10.1029/2011WR010534.

941 Yi, L.X., Zhang, F., Xu, H., Chen, S.J., Wang W., Yu, Q., 2011. Land subsidence in Tianjin,
942 China. *Environ. Earth Sci.* 62, 1151–1161. doi: 10.1007/s12665-010-0604-5.

943 Zhao, B., Nie, Z.S., Huang, Y., Wang, W., Zhang, C.H., Tan, K., Du, R.L., 2014. Vertical
944 motion of north China inferred from dense GPS measurements. *J. Geodesy Geodyn.* 34 (5),
945 35–39 (in Chinese with an English abstract).

946 [Zhong, M., Duan, J.B., Xu, H.Z., Peng, P., Yan, H.M., Zhu, Y.Z., 2009. Trend of China land](#)
947 [water storage redistribution at medi- and largespacial scales in recent five years by satellite](#)
948 [gravity observations. Chin. Sci. Bull., 54\(5\), 816–821.](#)
949

950 **Table captions:**

951 **Table 1.** GPS Station information.

952

953 **Table 2.** Trends of ~~GRACE-TWS~~ derived ~~TWS by GRACE~~ and ~~GWS (sealed-GRACE minus~~
954 ~~GLDAS/Noah), in situ measurements (shallow aquifers) and compare with the previous~~
955 ~~studies~~ during 2003-~~2009~~ and 2003-2012.

956

957 **Figure captions:**

958 **Figure 1.** Study region of North Plain China (NCP) showing locations of continuous GPS
959 stations. White dots represent continuous GPS sites in the Crustal Movement Observation
960 Network of China (CMONOC) and red stars represent the International GNSS Service (IGS)
961 sites). Cities and provinces are labeled as follows: Beijing (BJ), Tianjin (TJ), Hebei province
962 (HE), and Shanxi province (SX).

963

964 **Figure 2.** The 2003–2012 secular trend maps (cm/yr) of the terrestrial water storage (TWS)
965 changes in North Plain China (NCP) and surrounding regions derived from GRACE data.
966 Results have been destriped and smoothed with a 250-km Gaussian smoothing function.

967

968 **Figure 3.** Daily values of the vertical (positive upward) components of position, as measured
969 at IGS GPS sites BJFS, ZHNS, BJSH, JIXN and TAIN. The example of displacement due to
970 atmospheric and non-tidal ocean loading at BJFS IGS sites are shown in (b).

971

972 **Figure 4.** Surface horizontal (north and east components) and vertical deformation modeled
973 by GRACE in four IGS sites. (a) and (b) show the time series and trend rates of north and east
974 components in BJFS, JIXN, TAIN and ZHNS, respectively, (c) show the time series of
975 vertical displacements.

976

977 **Figure 5.** Time series showing daily values (a) and fitting results (b) of the vertical (positive
978 upward) components from GPS and GRACE-derived at five IGS GPS sites.

979

980 **Figure 6.** Comparison of annual amplitudes and initial phases between GPS (grey) and
981 GRACE (red). The initial phases are counterclockwise from the east (reference time is
982 2004.0).

983

984 **Figure 7.** Time series showing total terrestrial water storage (TWS) changes in the spatially
985 averaged area (kernel) of the NCP estimated from CSR GRACE data, monthly groundwater
986 level changes observed by monitoring wells after multiplying by mean value of specific yields
987 in the NCP during 2002~2012 and the daily precipitation data (rainfall amount) for weather
988 stations during the period of 2003~2012 from CMDSSS. The black dashed curve is the
989 temporal smoothing GRACE-based result, the red and blue dashed curve are the long trend of
990 GRACE-based result during 2003~2009 and 2003~2012, respectively. The dashed curve is
991 the temporal smoothing result.

992

993 **Figure 8.** GRACE-derived smoothed (dash curves) and long-term (solid curves) vertical
994 displacement time series due to load changes (a), the groundwater depletion contributions
995 estimated from GRACE minus GLDAS data for smoothed (dash curves) and long-term (solid
996 curves) vertical displacements (b), as measured at five IGS stations and twenty CMONOC
997 stations ~~25 GPS sites~~ in NCP and its surrounding region. The grey background highlight part
998 shows inflexion effects due to TWS changes in the vertical component.

999

1000 **Figure 9.** Smoothed (dash curves) and long-term (solid curves) versions of daily values of the

1001 vertical (positive upward) component of position, as measured at ~~twenty nine~~²⁹ GPS sites in
1002 NCP and its surrounding region, (a) ~~five~~⁵ IGS stations and (b) ~~twenty four~~²⁴ CMONOC
1003 stations.

1004

1005 **Figure 10.** GPS (gray arrow, positive upward) and corrected GPS (red arrow, positive upward)
1006 vertical trend rate after subtracting the GRACE-derived long-term uplift rate due to load
1007 changes and GIA effect between 2004 and 2009 (a), and between 2010 and 2013 (b).

1008

1009 **Table 1:**
1010

Stations	Lat.	Lon.	Time	Annual Amplitude of vertical displacement (mm)		Annual Phase of vertical displacement (days) Reference time is 2004.0		Trend Rates of vertical displacement (mm/yr) 2004-2009		Trend Rates of vertical displacement (mm/yr) 2010-带格式表格	
				GPS	GRACE	GPS	GRACE	GPS	GRACE	GPS	GRACE
BJFS [*]	39.6	115.8		2.50±0.26	1.35±0.24	40.09±6.39	359.63±10.73	1.47±0.14	0.58±0.06	-0.37±0.23	带格式表格
BJSH [*]	40.2	116.2		3.25±0.23	1.25±0.23	52.75±4.20	1.00±11.09	0.12±0.12	0.53±0.06	-0.94±0.25	0.14±0.13
JIXN [*]	40	117.5	2003	2.46±0.22	1.32±0.23	32.20±5.11	359.72±10.56	1.21±0.12	0.53±0.06	-0.19±0.20	0.09±0.13
TAIN [*]	36.2	117.1	~2013	3.31±0.32	2.07±0.39	16.44±5.66	349.43±11.36	0.18±0.15	0.80±0.09	0.46±0.31	0.04±0.16
ZHNZ [*]	34.5	113.1		2.38±0.36	2.24±0.43	28.18±8.94	354.76±11.39	0.04±0.15	0.65±0.10	2.55±0.32	= -0.35±0.17
BJGB [#]	40.6	117.1		3.61±0.41	1.25±0.23	32.07±6.58	4.25±11.11		0.49±0.06	0.25±0.34	0.02±0.13
BJYQ [#]	40.3	115.9		3.55±0.41	1.23±0.23	25.82±6.87	3.34±11.26		0.52±0.06	-0.41±0.34	0.14±0.13
HAHB [#]	35.6	114.5		3.44±0.42	2.13±0.42	24.12±6.93	349.19±11.79		0.77±0.10	-0.55±0.27	= -0.28±0.17
HAJY [#]	35.1	112.4		2.28±0.51	2.05±0.44	9.28±13.00	355.65±12.80		0.84±0.10	-0.30±0.33	= -0.40±0.17
HECC [#]	40.8	115.8		2.49±0.39	1.17±0.23	9.25±9.05	11.15±11.81		0.49±0.06	1.32±0.25	0.06±0.13
HECD [#]	41	117.9		4.09±0.36	1.27±0.23	40.28±5.21	7.63±11.09		0.45±0.06	-0.68±0.25	= -0.07±0.13
HECX [#]	38.4	116.9		4.57±0.51	1.62±0.29	41.20±6.82	348.56±10.80		0.73±0.07	= -20.85±0.38	0.26±0.14
HELQ [#]	38.2	114.3		2.06±0.37	1.67±0.28	30.89±10.63	354.34±9.95		0.68±0.07	1.76±0.26	0.31±0.14
HELY [#]	37.3	114.7		2.65±0.37	1.88±0.33	10.54±8.44	350.61±10.56		0.79±0.08	0.30±0.27	0.11±0.15
HETS [#]	39.7	118.2		1.59±0.42	1.39±0.24	279.75±15.31	355.30±10.28		0.53±0.06	3.70±0.32	0.07±0.13
HEY [#]	40.1	114.1	2010	3.40±0.39	1.20±0.23	2.92±6.44	7.32±11.44		0.49±0.06	0.76±0.30	0.29±0.13
HEZJ [#]	40.8	114.9	~2013	1.95±0.35	1.13±0.23	364.91±10.74	15.62±12.11		0.47±0.06	1.06±0.25	0.11±0.13
NMTK [#]	40.2	111.2		3.37±0.47	1.02±0.23	8.85±7.09	25.83±13.67		0.37±0.06	1.20±0.37	0.51±0.13
NMZL [#]	42.2	115.9		1.72±0.39	1.15±0.23	37.43±14.85	30.16±12.06		0.41±0.06	-0.49±0.28	= -0.10±0.13
SDJX [#]	35.4	116.3		2.36±0.40	2.22±0.41	39.05±9.97	350.76±11.00		0.71±0.10	0.78±0.33	= -0.07±0.17
SDZB [#]	36.8	117.9		3.59±0.44	1.90±0.37	25.65±6.87	347.50±11.50		0.79±0.09	-1.12±0.30	0.12±0.16
SXCZ [#]	36.2	113.1		3.99±0.47	1.93±0.39	35.27±6.48	352.64±12.24		0.87±0.09	0.22±0.30	= -0.22±0.16
SXGX [#]	36.2	111.9		1.17±0.51	1.81±0.39	311.44±26.46	359.06±12.86		0.92±0.09	3.17±0.38	= -0.17±0.16
SXLF [#]	36	111.3		3.65±0.48	1.79±0.40	18.16±7.77	363.02±13.33		0.95±0.10	1.21±0.31	= -0.19±0.17
SXLQ [#]	39.3	114		3.63±0.47	1.38±0.24	25.49±7.95	362.70±10.45		0.54±0.06	1.42±0.33	0.39±0.13
SXXX [#]	35.1	111.2		2.93±0.54	1.98±0.43	15.09±10.44	363.17±13.18		0.90±0.10	1.30±0.41	=

TJBD [#]	39.6	117.3	3.36±0.48	1.38±0.24	25.80±7.38	355.65±10.54	0.58±0.06	-1.10±0.33	-0.36±0.17
TJBH [#]	39	117.6	6.25±0.45	1.49±0.26	42.18±9.56	350.10±10.60	0.64±0.06	-16.84±0.37	0.20±0.13
TJWQ [#]	39.3	117.1	5.08±0.49	1.43±0.25	0.11±8.23	353.28±10.58	0.62±0.06	-44.46±0.45	0.21±0.13

1011 ^{*}IGS sites: the observation time between 2003 and 2013.

1012 [#]CMONOC sites: the observation time between 2010 and 2013.

1013

1014

1015

1016

1017

1018 **Table 2:**

1019

Time-Span	<u>TWS</u> 2003~2009GRAC E-Trend (cm/yr of the water thickness)	<u>TWS</u> 2003~2012GRAC E Scaled ($\times 1/0.47$) Trend (cm/yr of the water thickness)	<u>GWS</u> 2003~2009GRACE Scaled ($\times 3.6626/0.47$) Trend (km^3/yr of the mass)	<u>GWS</u> 2003~2012 Trend
^a This study 2003~2009	-1.62±0.39	1.23-3.39±0.2384	-1.17±0.41-12.42±3.15	1.28±0.25
^a This study 2003~2012 multiplied by a scaling factor=1 (cm)/0.47 (cm)	3.39-1.23±0.8123	-2.57±0.49	-2.49±0.9.41±1.79	2.72±0.25
^b This study after multiplied by a scaling factor=3.6626 (km^3)/0.47 (cm)	-12.42±3.15	-9.41±1.79	-9.12±3.34 -9.96±1.95	
^a In situ measurements (shallow aquifers)			-1.57±0.31 -0.98±0.20	
^a Huang et al. (2015)			-2.83±0.71	
^a Feng et al.			-2.2±0.3	

带格式的：两端对齐

插入的单元格

带格式表格

带格式的：在相同样式的段落间不添加空格，行距：单倍行距

带格式的：字体：10.5 磅，检查拼写和语法

带格式的：在相同样式的段落间不添加空格，行距：单倍行距

带格式的：字体：10.5 磅，检查拼写和语法

	<u>(2013)</u>		<u>(2003~2010)</u>	
)	
^a <u>Tang et al.</u>				<u>-0.8~-1.4</u>
<u>(2013)</u>				<u>(2003~2011)</u>
)
^a <u>Su et al.</u>	<u>-1.1</u>		<u>-0.5</u>	
<u>(2011)</u>	<u>(2002~2010)</u>		<u>(2002~2010)</u>	
)	
^a <u>Moiwo et al.</u>	<u>-1.68</u>			
<u>(2009)</u>	<u>(2002~2009)</u>			
^a <u>Zhong et al.</u>	<u>-2.4</u>			
<u>(2009)</u>	<u>(2003~2007)</u>			

1020 ^a cm/yr of the water thickness

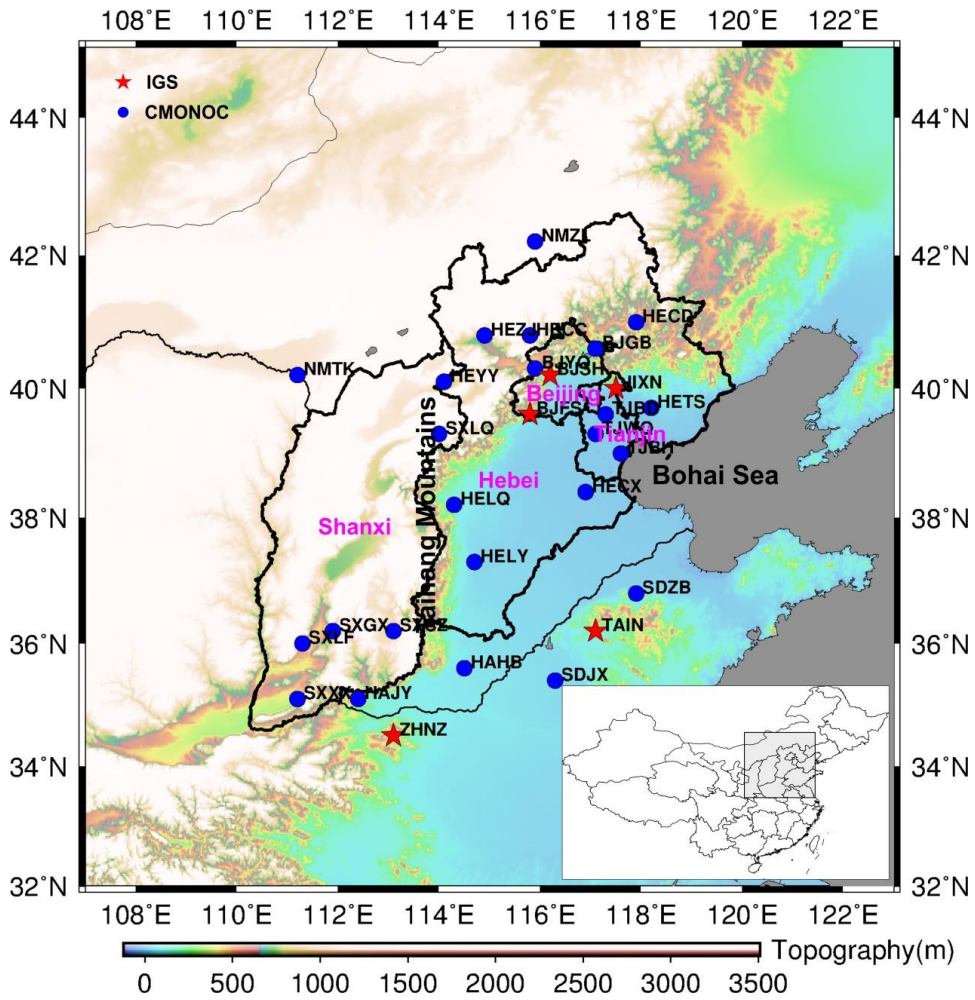
1021 ^b km³/yr of the mass

1022 ▲

带格式的: 字体: 10.5 磅

1023 **Figure 1:**

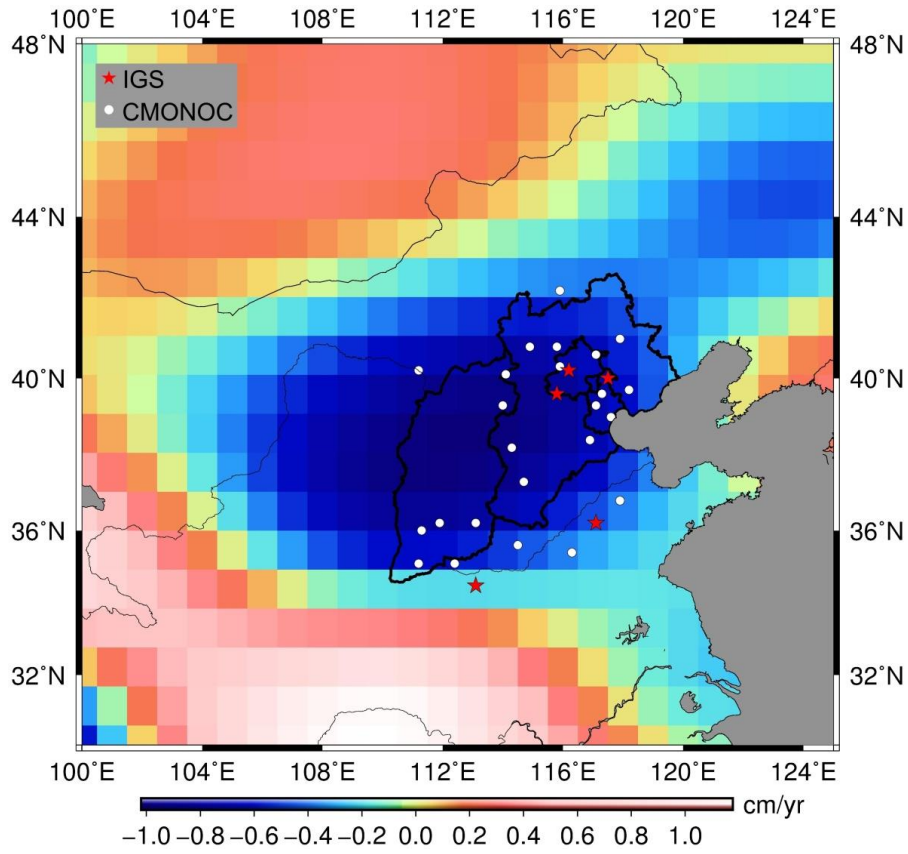
1024



1025

1026 **Figure 2:**

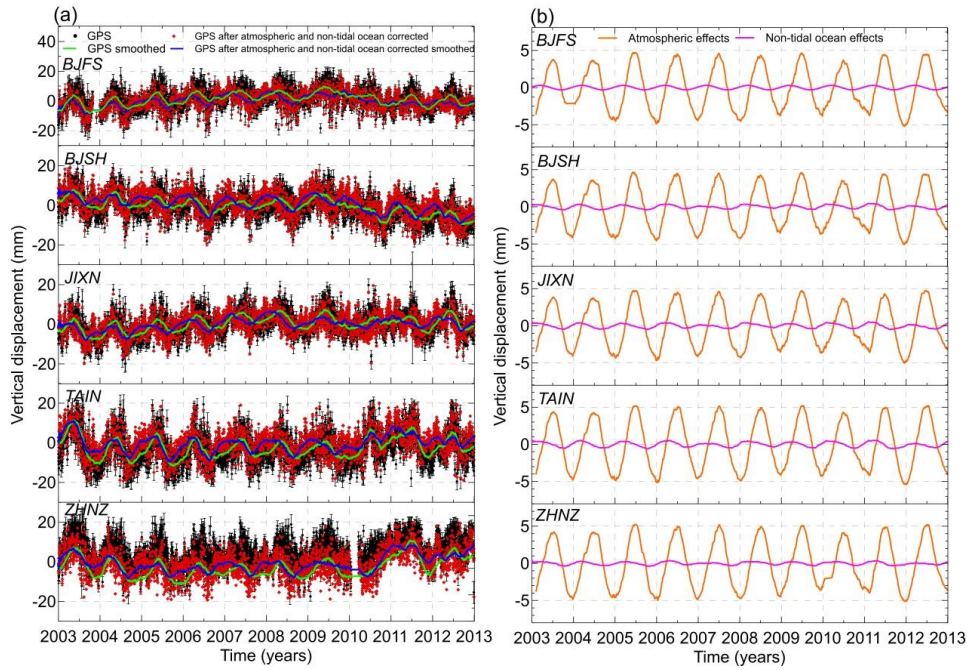
1027



1028

1029 **Figure 3:**

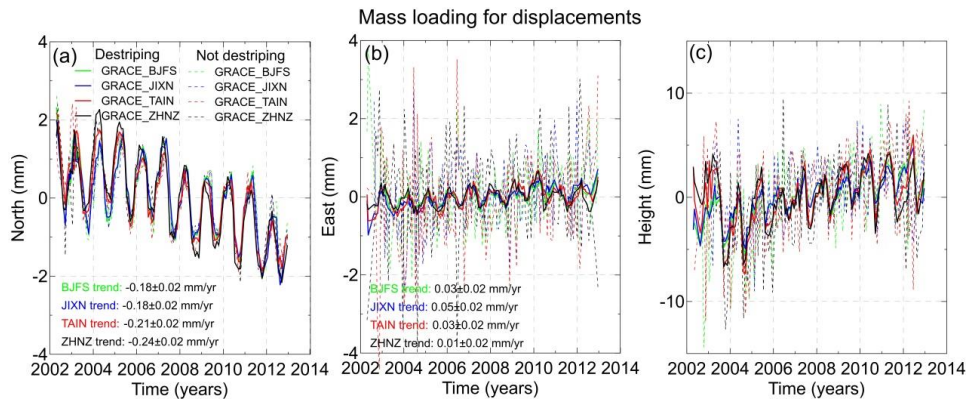
1030



1031

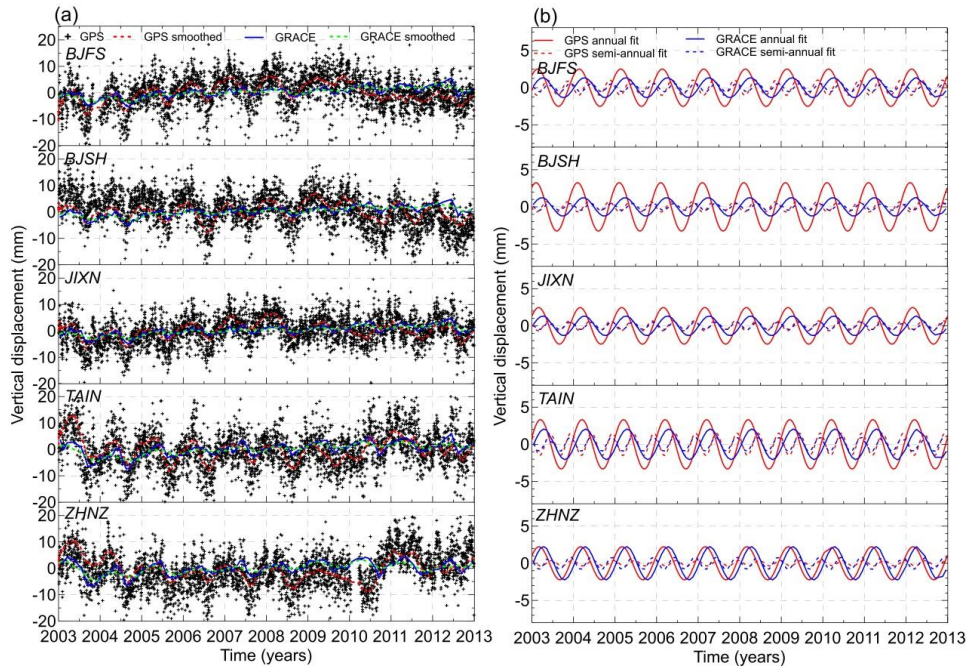
1032 **Figure 4:**

1033



1034

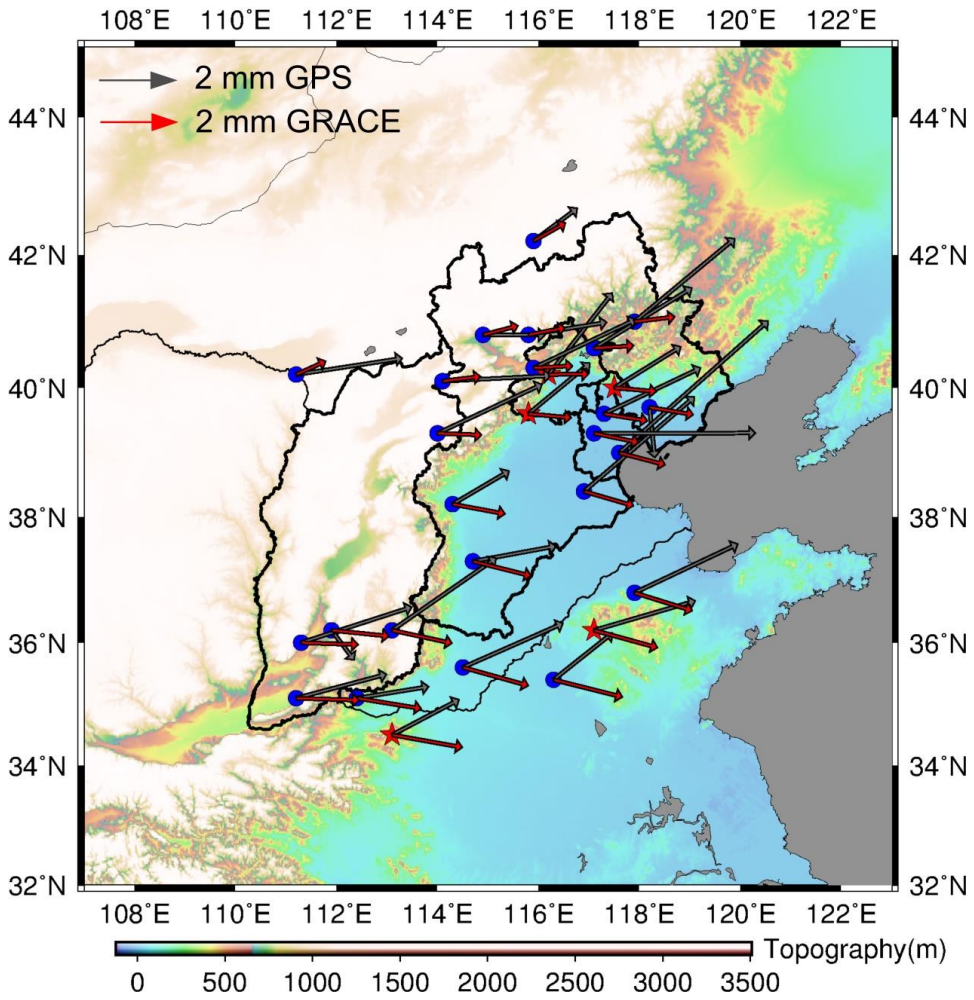
1035 **Figure 5:**



1036

1037 **Figure 6:**

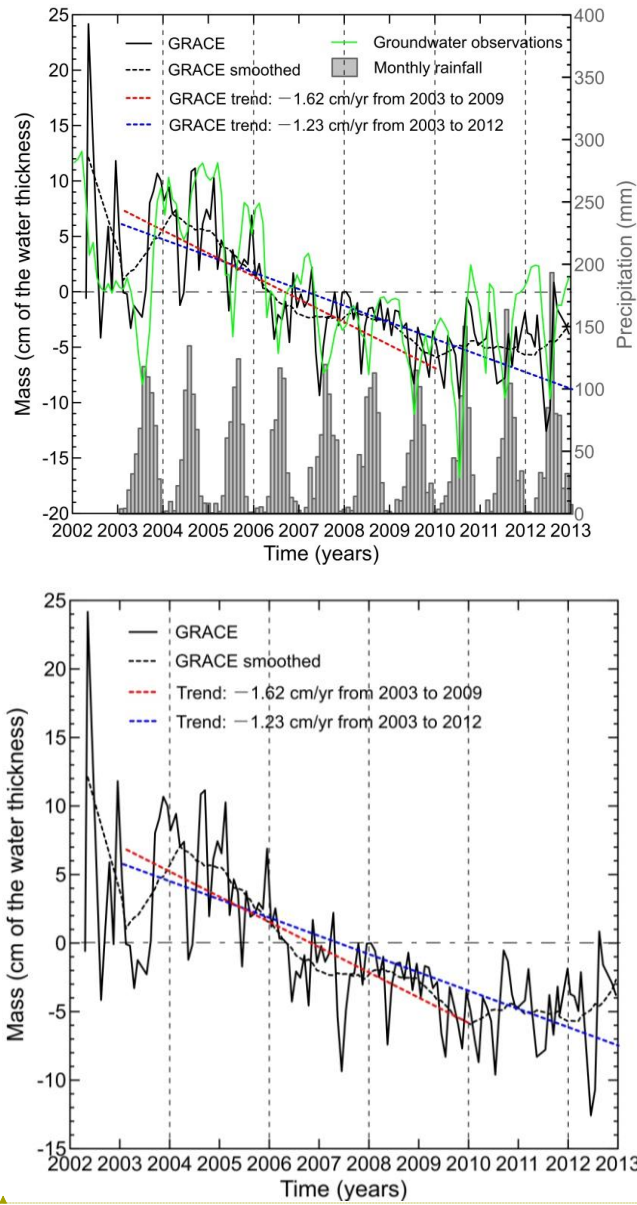
1038



1039

1040 **Figure 7:**

1041



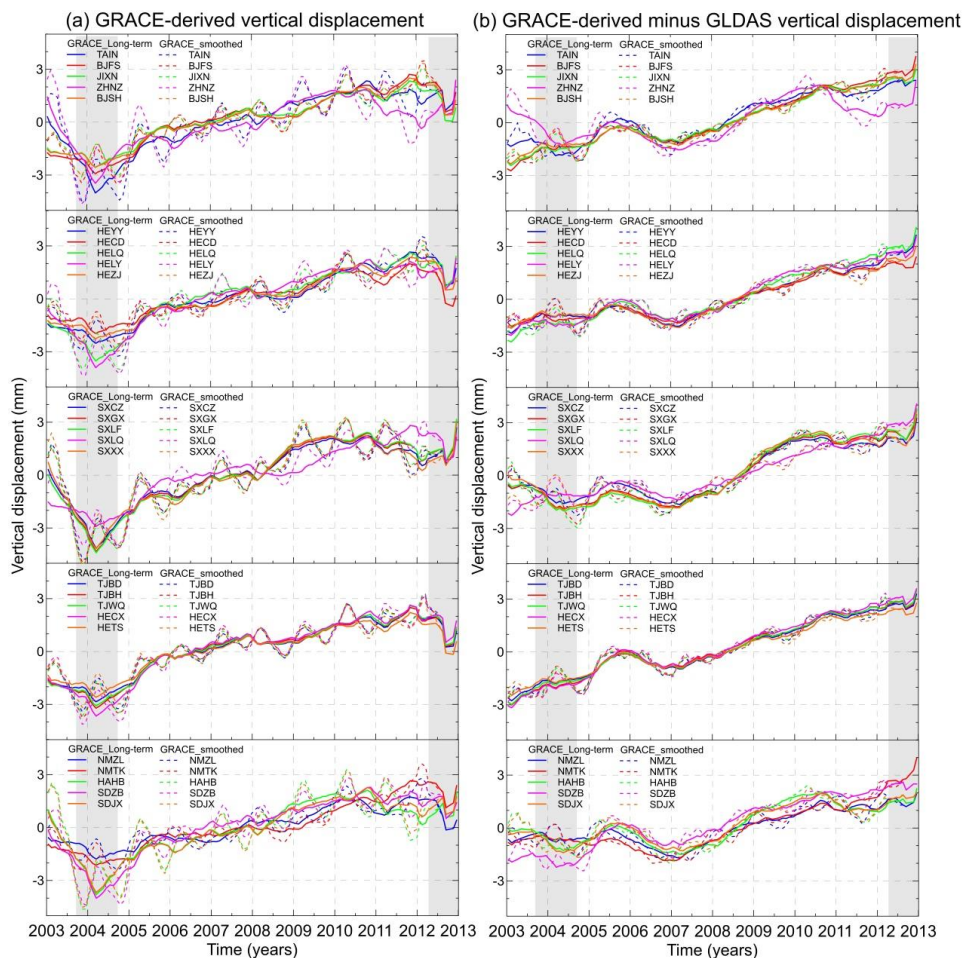
带格式的: 字体: Times New Roman, 12 磅

1042

1043

1044 **Figure 8:**

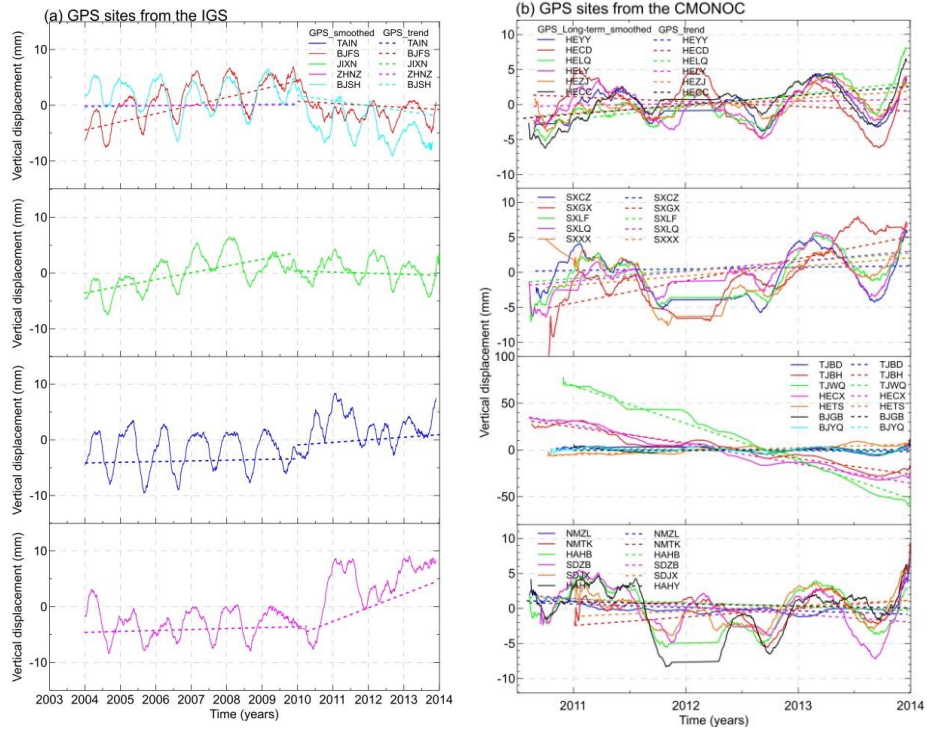
1045



1046

1047 **Figure 9:**

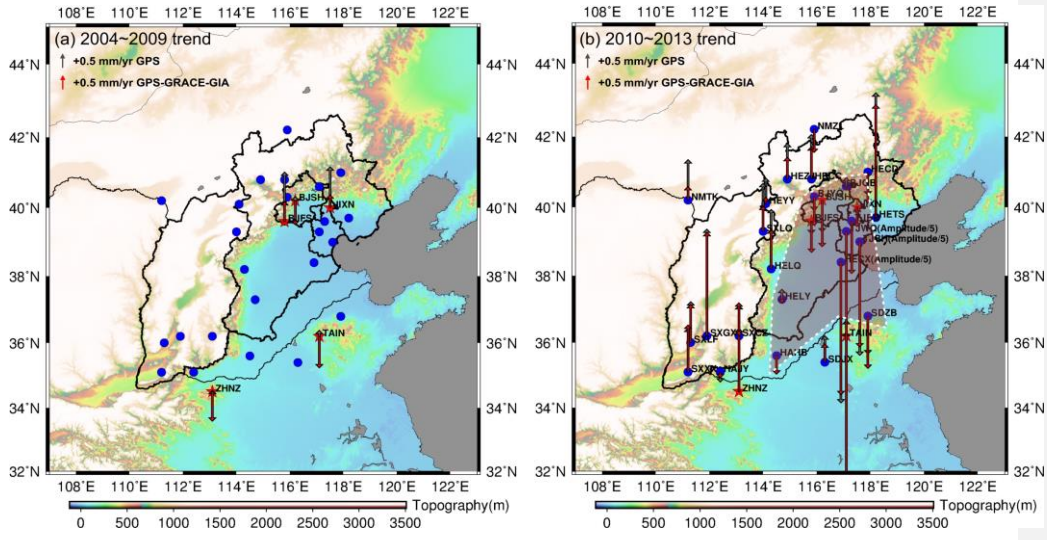
1048



1049

1050 **Figure 10:**

1051



1052

1053